Field Guide to

Atmospheric Optics

Larry C. Andrews
University of Central Florida

SPIE Field Guides
Volume FG02

John E. Greivenkamp, Series Editor

SPIE
PRESS

Bellingham, Washington USA

Published by

SPIE—The International Society for Optical Engineering
P.O. Box 10
Bellingham, Washington 98227-0010 USA
Phone: +1 360 676 3290
Fax: +1 360 647 1445
Email: spie@spie.org
Web: http://spie.org

Printed in the United States of America. Second printing 2007.

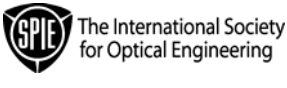

Introduction to the Series

Welcome to the *SPIE Field Guides*! This volume is one of the first in a new series of publications written directly for the practicing engineer or scientist. Many textbooks and professional reference books cover optical principles and techniques in depth. The aim of the *SPIE Field Guides* is to distill this information, providing readers with a handy desk or briefcase reference that provides basic, essential information about optical principles, techniques, or phenomena, including definitions and descriptions, key equations, illustrations, application examples, design considerations, and additional resources. A significant effort will be made to provide a consistent notation and style between volumes in the series.

Each *SPIE Field Guide* addresses a major field of optical science and technology. The concept of these *Field Guides* is a format-intensive presentation based on figures and equations supplemented by concise explanations. In most cases, this modular approach places a single topic on a page, and provides full coverage of that topic on that page. Highlights, insights and rules of thumb are displayed in sidebars to the main text. The appendices at the end of each *Field Guide* provide additional information such as related material outside the main scope of the volume, key mathematical relationships and alternative methods. While complete in their coverage, the concise presentation may not be appropriate for those new to the field.

The *SPIE Field Guides* are intended to be living documents. The modular page-based presentation format allows them to be easily updated and expanded. We are interested in your suggestions for new *Field Guide* topics as well as what material should be added to an individual volume to make these Field Guides more useful to you. Please contact us at fieldguides@SPIE.org.

John E. Greivenkamp, *Series Editor*
Optical Sciences Center
The University of Arizona

The Field Guide Series

Keep information at your fingertips with all of the titles in the Field Guide Series:

Field Guide to Geometrical Optics, John E. Greivenkamp (FG01)

Field Guide to Atmospheric Optics, Larry C. Andrews (FG02)

Field Guide to Adaptive Optics, Robert K. Tyson and Benjamin W. Frazier (FG03)

Field Guide to Visual and Ophthalmic Optics, Jim Schwiegerling (FG04)

Field Guide to Polarization, Edward Collett (FG05)

Field Guide to Optical Lithography, Chris A. Mack (FG06)

Field Guide to Optical Thin Films, Ronald R. Willey (FG07)

Field Guide to Spectroscopy, David W. Ball (FG08)

Field Guide to Infrared Systems, Arnold Daniels (FG09)

Field Guide to Interferometric Optical Testing, Eric P. Goodwin and James C. Wyant (FG10)

Field Guide to Atmospheric Optics

The material in this *Field Guide* is a condensed version of similar material found in two textbooks: *Laser Beam Propagation through Random Media* by L. C. Andrews and R. L. Phillips and *Laser Beam Scintillation with Applications* by L. C. Andrews, R. L. Phillips, and C. Y. Hopen. Both books are SPIE Press publications.

Topics chosen for this volume include a review of classical Kolmogorov turbulence theory, Gaussian-beam waves in free space, and atmospheric effects on a propagating optical wave. These atmospheric effects have great importance in a variety of applications like imaging, free space optical communications, laser radar, and remote sensing. Specifically, we present tractable mathematical models from which the practitioner can readily determine beam spreading, beam wander, spatial coherence radius (Fried's parameter), angle-of-arrival fluc-tuations, scintillation, aperture averaging effects, fade probabilities, bit error rates, and enhanced backscatter effects, among others.

Notation used in this field guide is largely based on common usage found in propagation studies but may be different from that commonly used in related areas. For example, the symbol "I" is used here for irradiance. In the radiometry community, the symbol "E" is commonly used for irradiance (W/m^2) and the symbol "I" is reserved for intensity (W/sr).

The foundational material for atmospheric optics has generally been widely dispersed throughout the journal literature over many years, making it difficult for researchers to update their knowledge and for newcomers to the field to compile and understand this difficult subject area. It is hoped that this *Field Guide* will serve a useful purpose for practicing engineers and scientists who wish to have access to such material in a single concise presentation.

Larry C. Andrews
University of Central Florida

Table of Contents

Glossary of Symbols

A	Aperture averaging factor
$b_I(\rho, L)$	Normalized covariance function of irradiance
BER	Bit error rate
$B_I(\mathbf{r}_1, \mathbf{r}_2, L), B_I(\rho)$	Covariance function of irradiance
$B_I^{iR}(\mathbf{r}, L)$	Correlation function associated with amplitude enhancement of reflected wave
c	Speed of light ($= 3 \times 10^8$ m/s)
$C_n^2, C_n^2(h)$	Refractive-index structure parameter
C_V^2	Velocity structure parameter
C_T^2	Temperature structure parameter
CNR	Carrier-to-noise ratio
d	Normalized lens diameter ($= \sqrt{kD^2/4L}$)
D	Diameter of collecting lens
DOC	Modulus of the complex degree of coherence
$D(\mathbf{r}_1, \mathbf{r}_2, L), D(\rho, L)$	Wave structure function
$D_S(\rho, L)$	Phase structure function
$D_n(R)$	Index of refraction structure function
$D_{RR}(R)$	Velocity structure function
$D_T(R)$	Temperature structure function
E	Electric field
erf(x), erfc(x)	Error functions
EBS	Enhanced backscatter
EG	Equal gain coherent detection scheme
EO	Electro-optics
F	Phase front radius of curvature of beam at receiver
FAR	False alarm rate
F_G	Effective focal length of Gaussian lens
F_T	Fade level (in dB) below the mean on-axis irradiance
F_0	Phase front radius of curvature of beam at transmitter

Glossary of Symbols (cont'd)

${}_pF_q$	Generalized hypergeometric function
$G(\mathbf{s}, \mathbf{r}; L)$	Green's function
h	Altitude
h_0	Altitude of transmitter/receiver
H	Altitude of receiver/transmitter
$H_n(x)$	Hermite polynomial of degree n
$H - V_{5/7}$	Hufnagle-Valley $C_n^2(h)$ model
i_{IF}	Intermediate frequency (IF) signal current
i_S	Signal current in a receiver
i_N	Shot noise current in a receiver
i_T	Current threshold in a receiver
$I^0(\mathbf{r}, L)$	Irradiance of beam in free space
$I(\mathbf{r}, L)$	Irradiance of beam in random medium
$I_v(x)$	Modified Bessel function of order v
$J_v(x)$	Bessel function of order v
k	Wave number of beam wave $(= 2\pi/\lambda)$
$K_v(x)$	Modified Bessel function of order v
l_0	Inner scale of turbulence
L	Propagation path length
LO	Local oscillator
L_0	Outer scale of turbulence
$L_n^{(m)}(x)$	Associated Laguerre polynomial
MCF	Mutual coherence function
MTF	Modulation transfer function
$n(\mathbf{R})$	Index of refraction
$n_1(\mathbf{R})$, $n_1(\mathbf{r}, z)$	Random fluctuation in index of refraction
OTF	Optical transfer function
$\mathbf{p}$	Transverse vector between two observation points
$p_I(I)$	Probability density function of irradiance
PSF	Point spread function
$\mathrm{Pr_d}$	Probability of detection

$\mathrm{Pr}_{\mathrm{fa}}$	Probability of false alarm
$\mathrm{Pr}(E)$	Probability of error
P_S	Signal power
q	Strength of turbulence parameter ($=L/k\rho_0^2$)
Q_l	Nondimensional inner-scale parameter ($=L\kappa_l^2/k$)
Q_0	Nondimensional outer-scale parameter ($=L\kappa_0^2/k$)
$\mathbf{r}$	Transverse position of observation point
r_0	Atmospheric coherence length (Fried's parameter)
$\mathbf{R}$	Position vector in three dimensions
Re	Reynolds number
$S(\mathbf{r}, L)$	Random phase
$S_I(\omega)$	Power spectral density of irradiance
SNR	Signal-to-noise ratio
SR	Strehl ratio
TEM_{mn}	Transverse electromagnetic mode
$U_0(\mathbf{r}, z)$	Complex amplitude of the field in free space
$U(\mathbf{r}, z)$	Complex amplitude of the field in random medium
W_0	Beam radius at transmitter
W	Beam radius in free space at receiver
W_B	Beam radius in free space at the waist
W_e	Effective beam radius in random medium at receiver
W_G	Radius of Gaussian lens
W_R	Radius of target (reflector) surface
WSF	Wave structure function
z_B	Distance to beam waist from transmitter
$Z_n^m(r, \theta), Z_i[m, n]$	Zernike polynomials

Glossary of Symbols (cont'd)

$\alpha(L)$	Extinction coefficient
α, β	Parameters of the gamma-gamma distribution
β_0^2	Rytov variance for a spherical wave
$\Gamma(x)$	Gamma function
$\Gamma_2(\mathbf{r}_1, \mathbf{r}_2, L)$	Mutual coherence function
$\Gamma_4(\mathbf{r}_1, \mathbf{r}_2, \mathbf{r}_3, \mathbf{r}_4, L)$	Fourth-order moment of the field
θ_0	Isoplanatic angle
Θ_0	Beam curvature parameter at transmitter
Θ	Beam curvature parameter at receiver
κ	Scalar spatial wave number
κ_l	Inner-scale wave number parameter $(= 3.3/l_0)$
κ_m	Inner-scale wave number parameter $(= 5.92/l_0)$
κ_0	Outer-scale wave number parameter $(= 2\pi/L_0)$
λ	Wavelength
Λ_0	Fresnel ratio of beam at transmitter
Λ	Fresnel ratio of beam at receiver
ρ	Scalar separation distance between two observation points
ρ_c	Correlation width of irradiance fluctuations
ρ_0	Transverse spatial coherence radius
σ_1^2	Rytov variance for a plane wave
σ_B^2	Rytov variance for a Gaussian-beam wave
σ_{diff}^2	Scintillation associated with reflected wave from a diffuse target
σ_I^2	Scintillation index (normalized irradiance variance)
$\sigma_I^2(D)$	Irradiance flux variance for a collecting aperture of diameter D
σ_N^2	Total noise power in detector current

$\Phi_n(\kappa)$	Three-dimensional spatial power spectrum of refractive index
$\Phi_{RR}(\kappa)$	Three-dimensional spatial power spectrum of velocity
$\Phi_T(\kappa)$	Three-dimensional spatial power spectrum of temperature
$\chi(\mathbf{r}, L)$	Random log-amplitude
$\psi_1(\mathbf{r}, L)$, $\psi_2(\mathbf{r}, L)$	Complex phase perturbations of Rytov approximation
$\psi_1(\mathbf{r}, \mathbf{s})$, $\psi_2(\mathbf{r}, \mathbf{s})$	Complex phase perturbations of extended Huygens-Fresnel principle
Ω_f	Focusing parameter for geometric focus
Ω_G	Fresnel ratio characterizing radius of Gaussian lens
Ω_R	Fresnel ratio characterizing radius of reflector target
ζ	Zenith angle
∇^2	Laplacian operator
∇^2_{T1}	Laplacian operator with respect to $\mathbf{r}_1$
∇^2_{T2}	Laplacian operator with respect to $\mathbf{r}_2$
$\langle\ \rangle$	Ensemble average

Atmospheric Structure

It is well known that rain, snow, sleet, fog, haze, pollution, etc., are atmospheric factors that affect our viewing of distant objects. These same factors can also affect the transmission of electromagnetic radiation through the atmosphere, particularly optical waves.

The three primary atmospheric processes that affect optical wave propagation are **absorption**, **scattering**, and **refractive-index fluctuations** (i.e., optical turbulence). Absorption and scattering by the constituent gases and particulates of the atmosphere give rise primarily to attenuation of an optical wave. Index of refraction fluctuations lead to **irradiance fluctuations**, **beam broadening**, and **loss of spatial coherence** of the optical wave, among other effects. Clearly, these deleterious effects have far-reaching consequences on astronomical imaging, optical communications, remote sensing, laser radar, and other applications that require the transmission of optical waves through the atmosphere.

Atmospheric Structure with Altitude

The atmosphere is a gaseous envelope that surrounds the earth and extends to several hundred kilometers above the surface. Based mostly on temperature variations, the earth's atmosphere is divided into four primary layers separated by three isothermal boundaries.

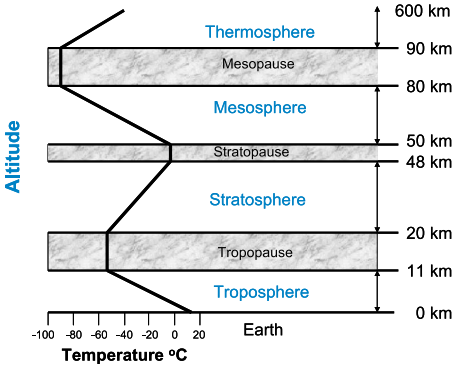

Troposphere: Contains roughly 75% of the earth's atmospheric mass. Maximum air temperature occurs near the surface of the earth, but decreases with altitude to −55°C. The **tropopause** is an isothermal layer where air temperature remains constant at −55°C.

Stratosphere: The air temperature in this layer increases with altitude because the ozone gas absorbs ultraviolet sunlight, thereby creating heat energy. The ozone layer, which protects life from harmful ultraviolet radiation, is concentrated between 10–50 km. Separating the mesosphere from the stratosphere is the **stratopause**, another isothermal layer.

Mesosphere: Temperature generally decreases at a constant rate down to −90°C, the coldest in the atmosphere. The **mesopause** is the third isothermal layer.

Thermosphere: Air temperature increases quite strongly above 90 km. This layer includes most of the **ionosphere** and the **exosphere**, the last being the outermost region of the atmosphere.

Absorption and Scattering

Absorption and **scattering** refer to wavelength-dependent attenuation of electromagnetic radiation. Absorption is fundamentally a quantum process where atmospheric molecules absorb energy from incident photons. Scattering results from photons colliding with atmospheric particles. The single scattering theories below are based on the assumption of spherical-shaped, non-interacting particles.

Water vapor, CO_2, NO_2, CO, and ozone are the primary radiation absorbers. Absorption by the ozone O_2 and O_3 essentially eliminates propagation of radiation when $\lambda < 0.2$ μm, but little absorption occurs at visible wavelengths (0.4 to 0.7 μm) except for H_2O absorption between 0.65 and 0.85 μm. Both CO_2 and water vapor are radiation absorbers at IR wavelengths.

Rayleigh scattering (after Lord Rayleigh) is caused by air molecules and haze that are small in comparison with the wavelength λ of the radiation. The scattering coefficient is proportional to λ^{-4}, known as the **Rayleigh law**. For air molecules, scattering is negligible at $\lambda > 3$ μm. At $\lambda < 1$ μm, Rayleigh scattering produces the blue color of the sky because blue light is scattered much more than red light.

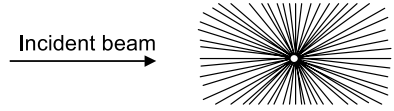

Rayleigh scattering

Mie scattering (after Gustav Mie) is scattering by particles comparable in size to the radiation wavelength (aka aerosol scattering). Scattering losses decrease rapidly with increasing wavelength, eventually approaching the Rayleigh scattering case. Mie scattering is the reason why sunsets appear red.

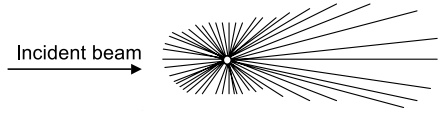

Mie scattering

Transmittance, Optical Depth, and Visibility

The **transmittance** of laser radiation that has propagated a distance L is described by **Beer's law**

$$\tau = \exp[-\alpha(\lambda)L]. \qquad \text{[unitless]}$$

Here, $\alpha(\lambda) = A_a + S_a$ is the **extinction coefficient**, where A_a is the absorption coefficient and S_a is the scattering coefficient. Extinction is defined as the attenuation in the amount of radiation passing through the atmosphere.

Software packages like LOWTRAN, FASCODE, MODTRAN, HITRAN, and PCLNWIN are commonly used to predict transmittance (attenuation) effects as a function of λ.

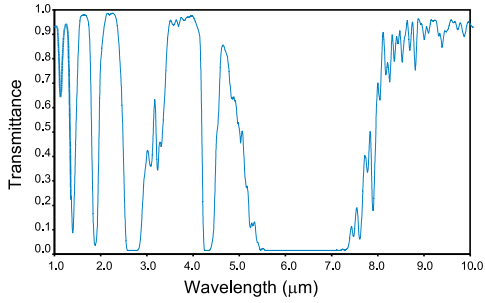

Typical atmospheric transmittance for a horizontal 1-km path. Height above ground is 3 m with no rain or clouds.

Optical depth is defined by the product $\alpha(\lambda)L$ appearing in the transmittance expression above.

Visibility (or **visual range**) corresponds to the range at which radiation at 0.55 μm is attenuated to 0.02 times its transmitted level. Rayleigh scattering by molecules implies a visual range of approximately 340 km (or 213 miles).

Meteorological Phenomena

Blue sky: Caused by the scattering of sunlight off air particles (molecules) that are small in comparison with the radiation wavelength.

Red sunset: Sunlight near the horizon must pass through a greater thickness of air than when the sun is overhead. Shorter-wavelength sunlight is therefore scattered more out of the beam by the additional aerosols and particulate matter, leaving only the longer red wavelength to get through to the observer.

Green flash: A rare phenomenon seen at sunrise and sunset when some part of the sun suddenly changes color from red or orange to green or blue. It occurs just before the last part of the sun disappears from view.

Green ray: A rare kind of green flash in which a beam of green light is seen shooting up from the horizon where the sun has just set.

Halo: Occurs around the sun in cold climates as a result of ice crystals in the air. The familiar 22° halo around the sun or moon occurs because of refraction in tiny hexagonal ice crystals in the air. The order of colors is reversed from that of diffraction (i.e., the inner circle is red).

Corona: A circle of light distinct from the 22° halo that can sometimes be seen around the sun or moon if there are thin clouds composed of water droplets or ice crystals of nearly uniform size. The appearance is often that of alternating blue-green and red circles.

Glory: A phenomenon seen from an aircraft. It involves a rainbow band around the shadow of your aircraft seen on a cloud below. It is another phenomenon of diffraction, with smaller droplets causing larger glories through Mie scattering.

Kolmogorov Theory of Turbulence

Classical studies of **turbulence** were concerned with fluctuations in the velocity field of a viscous fluid. In particular, it was observed that the longitudinal wind velocity associated with the turbulent atmosphere fluctuates randomly about its mean value. That is, the wind velocity field assumes the nature of a random or stochastic field, which means that at each point in space and time within the flow the velocity may be represented by a random variable.

A statistical approach has been fruitful over the years in describing both atmospheric turbulence and its various effects on optical/IR systems. For the purpose of mathematical simplification, it is often necessary in such statistical approaches to assume that point separations within certain scale sizes exhibit the important characteristics of statistical homogeneity and isotropy. In general, **statistical homogeneity** of the random velocity field implies that the mean value of the field is constant and that correlations between random fluctuations in the field from point to point are independent of the chosen observation points, depending only on their vector separation. Moreover, if the random fluctuations are also statistically **isotropic**, then point-to-point correlations depend only on the magnitude of the vector separation between observation points.

Classical Turbulence

Classical turbulence is associated with the random **velocity fluctuations** of a viscous fluid such as the atmosphere. The atmosphere has two distinct states of motion: laminar and turbulent. Mixing does not occur in **laminar flow**, but **turbulent flow** is characterized by dynamic mixing and acquires random subflows called **turbulent eddies**.

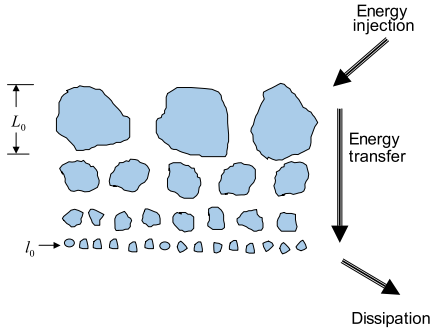

Reynolds number: $Re = Vl/\nu$, where V [m/s] and l [m] are the velocity (speed) and "dimension" of the flow, and ν [m^2/s] is the kinematic viscosity. Transition from laminar to turbulent flow takes place at a **critical Reynolds number**. Close to the ground $Re \sim 10^5$, considered highly turbulent.

Kolmogorov turbulence theory is the set of hypotheses that a small-scale structure is statistically homogeneous, isotropic, and independent of the large-scale structure. The source of energy at large scales is either wind shear or convection. When the wind velocity is sufficiently high that the critical Reynolds number is exceeded, large unstable air masses are created.

Energy cascade theory—unstable air masses under the influence of inertial forces break up into smaller eddies to form a continuum of eddy size for the transfer of energy from a macroscale L_0 (**outer scale of turbulence**) to a microscale l_0 (**inner scale of turbulence**).

Inertial range—family of eddies bounded by L_0 above and l_0 below.

Dissipation range—scale sizes smaller than l_0. The remaining energy in the fluid motion is **dissipated as heat**.

Velocity Fluctuations

Velocity structure function of wind velocity satisfies the power laws

$$D_{RR}(R) = \langle (V_1 - V_2)^2 \rangle = \begin{cases} C_V^2 R^{2/3}, & l_0 \ll R \ll L_0, \\ C_V^2 l_0^{-4/3} R^2, & R \ll l_0, \end{cases}$$

where V_1, V_2 denote the velocity at two points separated by distance R. Here, C_V^2 is the velocity **structure constant** (or **structure parameter** [units of $m^{4/3}/s^2$]), related to the average energy dissipation rate ϵ [units of m^2/s^3] by

$$C_V^2 = 2\epsilon^{2/3}.$$

In the surface layer up to ~100 m, L_0 is on the order of height above ground of the observation point. Only eddies of scale sizes smaller than L_0 are assumed **statistically homogeneous** and **isotropic**. As the turbulent eddies become smaller, the relative amount of energy dissipated by viscous forces increases until the energy dissipated matches that supplied by the kinetic energy of the parent flow. The associated eddy size then defines the inner scale of turbulence, typically on the order of 1 to 10 mm near the ground.

Inner scale, l_0: Related to energy dissipation rate ϵ and viscosity ν by $l_0 = (\nu^3/\epsilon)^{1/4}$. Strong turbulence has smaller inner scale and weak turbulence has larger inner scale.

Outer scale, L_0: Proportional to $\epsilon^{1/2}$; increases and decreases directly with the strength of turbulence. It is the distance over which the mean flow velocity changes appreciably.

Power spectrum: Equivalent to the 2/3 power law of the structure function in the inertial range in three dimensions

$$\Phi_{RR}(\kappa) = 0.033 C_V^2 \kappa^{-11/3}, \quad 1/L_0 \ll \kappa \ll 1/l_0.$$

The power spectrum exhibits a $-11/3$ power law, which corresponds to a 1D spectrum with a $-5/3$ power law.

Temperature Fluctuations

The basic ideas of velocity fluctuations have also been applied to passive scalars such as **potential temperature** θ, related to absolute temperature T by $\theta = T + \alpha_a h$, where α_a is the adiabatic rate of decrease of the temperature and h is height above the Earth's surface. An associated l_0 and L_0 of the small-scale temperature fluctuations form the lower and upper boundaries of the **inertial-convective range**.

Temperature structure function:

$$D_T(R) = \left\langle (T_1 - T_2)^2 \right\rangle = \begin{cases} C_T^2 R^{2/3}, & l_0 \ll R \ll L_0 \\ C_T^2 l_0^{-4/3} R^2, & R \ll l_0, \end{cases}$$

where T_1, T_2 are the temperature at two points separated by distance R; C_T^2 is the temperature **structure constant** [in $\mathrm{deg}^2/\mathrm{m}^{2/3}$]. (The structure "constant" is also referred to as the structure "parameter.")

Inner scale: $l_0 = 5.8(D^3/\epsilon)^{1/4}$,

where D is the diffusivity of heat in air (in m^2/s).

The three-dimensional **power spectrum** of temperature fluctuations takes the $-11/3$ power-law form

$$\begin{aligned} \Phi_T(\kappa) &= \frac{1}{4\pi} \beta \chi \epsilon^{-1/3} \kappa^{-11/3} \\ &= 0.033 C_T^2 \kappa^{-11/3}, \quad 1/L_0 \ll \kappa \ll 1/l_0, \end{aligned}$$

where β is the Obukhov-Corrsin constant and χ is the rate of dissipation of mean-squared temperature fluctuations.

The temperature spectrum at high wave numbers actually contains a small "bump" near $1/l_0$ that can have important consequences on a number of applications involving optical wave propagation.

Optical Turbulence

At a point $\mathbf{R}$ in space the **index of refraction** is written as

$$n(\mathbf{R}) = 1 + 79 \times 10^{-6}[P(\mathbf{R})/T(\mathbf{R})] = 1 + n_1(\mathbf{R}),$$

where $n(\mathbf{R})$ has been normalized by its mean value n_0, P is pressure, T is temperature, and the small dependence on optical wavelength λ is neglected. Temperature-induced fluctuations in the atmospheric refractive index is called **optical turbulence**, which has properties of **statistical homogeneity** and **isotropy** within the inertial subrange.

Refractive-index structure function:

$$D_n(R) = \left\langle [n(\mathbf{R}_1) - n(\mathbf{R}_2)]^2 \right\rangle = \begin{cases} C_n^2 R^{2/3}, & l_0 \ll R \ll L_0 \\ C_n^2 l_0^{-4/3} R^2, & R \ll l_0, \end{cases}$$

where $\mathbf{R}_1, \mathbf{R}_2$ denote the refractive index at two points separated by distance R, and $\langle\ \rangle$ is an ensemble average.

Refractive-index inner scale: $l_0 = 7.4(\nu^3/\epsilon)^{1/4}$.

The **structure constant** C_n^2 [units of $\mathrm{m}^{-2/3}$] can be deduced from the temperature structure constant C_T^2 by

$$C_n^2 = (79 \times 10^{-6} P/T^2)^2 C_T^2.$$

The **power spectral density** for refractive-index fluctuations over the inertial subrange is defined by

$$\Phi_n(\kappa) = 0.033 C_n^2 \kappa^{-11/3}, \quad 1/L_0 \ll \kappa \ll 1/l_0.$$

The **Kolmogorov spectrum** is widely used in theoretical calculations. However, it is limited to the **inertial subrange** ($1/L_0 \ll \kappa \ll 1/l_0$) so other models of the spectrum for refractive-index fluctuations are required in some calculations.

Structure Parameter and Inner Scale

The **structure parameter** C_n^2 is a measure of turbulence strength.

Inner scale l_0 has a strong impact on scintillation.

Path-averaged values of C_n^2 and l_0 can be obtained simultaneously by optical measurements over a short path length (typically ~150 m) using a **scintillometer**.

Near ground level, C_n^2 data over a 24-hr period would show a diurnal cycle with peaks during midday hours, near constant values at night, and minima near sunrise and sunset.

Weak turbulence: $C_n^2 \sim 10^{-17}$ m$^{-2/3}$ or less

Strong turbulence: $C_n^2 \sim 10^{-13}$ m$^{-2/3}$ or more

For **vertical** or **slant paths** the structure parameter C_n^2 varies as a function of height above ground and must be described by an altitude profile model. Formulated from a series of measurements made over many years, several such models have now been developed, most based on specific geographic locations.

Inner scale values range in size from 1–2 mm up to 1 cm or more near the ground. Also, the inner-scale size increases and decreases inversely with the structure parameter C_n^2.

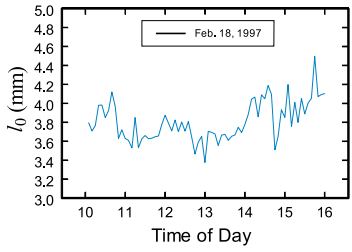

Measured values of the inner scale.

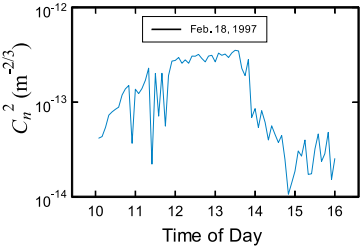

Measured values of C_n^2.

C_n^2 Profile Models

For applications involving propagation along a horizontal path, assume C_n^2 is constant. Propagation along a **vertical** or **slant path**, however, requires a C_n^2 profile model as a function of altitude h.

Hufnagle-Valley Model: one most often used by researchers

$$C_n^2(h) = 0.00594(w/27)^2(10^{-5}h)^{10}\exp(-h/1000) + 2.7\times 10^{-16}\exp(-h/1500) + A\exp(-h/100),$$

where $A = C_n^2(0)$ is a ground-level value of C_n^2, and w is **rms wind speed** often modeled by

$$w = \left[\frac{1}{15\times 10^3}\int_{5\times 10^3}^{20\times 10^3}\left\{\omega_s h + w_g + 30\exp\left[-\left(\frac{h-9400}{4800}\right)^2\right]\right\}^2 dh\right]^{1/2}.$$

Here, w_g is the ground wind speed and ω_s is the beam **slew rate**.

Two additional proposed models are given below.

SLC Day Model—

$$\begin{aligned} C_n^2(h) &= 1.7\times 10^{-14}, && 0 < h < 18.5 \text{ m},\\ &= 3.13\times 10^{-13}/h^{1.05}, && 18.5 < h < 240 \text{ m},\\ &= 1.3\times 10^{-15}, && 240 < h < 880 \text{ m},\\ &= 8.87\times 10^{-7}/h^3, && 880 < h < 7200 \text{ m},\\ &= 2.0\times 10^{-16}/h^{1/2}, && 7200 < h < 20000 \text{ m}. \end{aligned}$$

SLC Night Model—

$$\begin{aligned} C_n^2(h) &= 8.4\times 10^{-15}, && 0 < h < 18.5 \text{ m},\\ &= 2.87\times 10^{-12}/h^2, && 18.5 < h < 110 \text{ m},\\ &= 2.5\times 10^{-16}, && 110 < h < 1500 \text{ m},\\ &= 8.87\times 10^{-7}/h^3, && 1500 < h < 7200 \text{ m},\\ &= 2.0\times 10^{-16}/h^{1/2}, && 7200 < h < 20000 \text{ m}. \end{aligned}$$

Power Spectrum Models

Power spectrum: The Fourier transform of the refractive-index covariance function.

Kolmogorov spectrum: The conventional model for refractive-index fluctuations; theoretically valid only over the inertial subrange $1/L_0 \ll \kappa \ll 1/l_0$.

Tatarskii spectrum: For wavenumbers $\kappa > 1/l_0$, based on

$$\Phi_n(\kappa) = 0.033 C_n^2 \kappa^{-11/3} \exp(-\kappa^2/\kappa_m^2), \quad \kappa \gg 1/L_0,$$

where $\kappa_m = 5.92/l_0$. For $\kappa < 1/L_0$, the spectrum is **anisotropic** and its form is not known.

Von Kármán spectrum: For $\kappa < 1/L_0$, based on

$$\Phi_n(\kappa) = 0.033 C_n^2 \times \frac{\exp(-\kappa^2/\kappa_m^2)}{(\kappa^2 + \kappa_0^2)^{11/6}}, \quad 0 \le \kappa < \infty,$$

where $\kappa_0 = 2\pi/L_0$.

None of these models contain the rise ("bump") at high wave numbers near $1/l_0$ that appears in temperature spectral data.

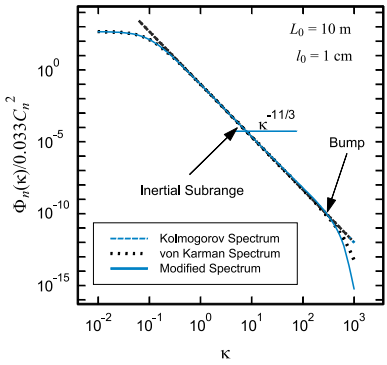

Several power spectum models for inner-scale $l_0 = 1$ cm and outer-scale $L_0 = 10$ m.

Modified atmospheric spectrum: An analytic approximation to the bump spectrum is given by

$$\Phi_n(\kappa) = 0.033 C_n^2 \left[1 + 1.802(\kappa/\kappa_l) - 0.254(\kappa/\kappa_l)^{7/6}\right] \times \frac{\exp(-\kappa^2/\kappa_l^2)}{(\kappa^2 + \kappa_0^2)^{11/6}}, \quad 0 \le \kappa < \infty,$$

where $\kappa_l = 3.3/l_0$, $\kappa_0 = 2\pi/L_0$.

Optical Wave Models in Free Space

There are several basic geometries commonly used to describe various optical/IR wave models. These include the infinite **plane wave**, **spherical wave**, and **Gaussian-beam wave**. The Gaussian-beam wave model used most often is the lowest-order transverse electromagnetic (TEM) wave, often denoted by TEM_{00}. Limiting cases of the TEM_{00} Gaussian-beam wave led to the infinite plane wave and spherical wave models. In practice, however, there are certain scenarios when it is desirable to minimize the excitation of nonlinearities within the crystal of a laser or when the received optical wave needs to have a multiple spot pattern. In those cases, the higher-order solutions of the paraxial wave equation can be used to generate **higher-order Gaussian-beam modes** with Hermite polynomials (CO_2 laser) in rectangular coordinates or Laguerre polynomials (HeNe laser) in cylindrical coordinates.

Paraxial Wave Equation

The **field** $E(\mathbf{R}, t)$ of a transverse electromagnetic TEM wave is a function of space $\mathbf{R} = (x, y, z)$ and time t that satisfies a partial differential equation.

Wave equation:

$$\nabla^2 E = \frac{\partial^2 E}{\partial x^2} + \frac{\partial^2 E}{\partial y^2} + \frac{\partial^2 E}{\partial z^2} = \frac{1}{c^2}\frac{\partial^2 E}{\partial t^2},$$

where the constant $c = 3 \times 10^8$ m/s is the speed of light.

Helmholtz equation (or **reduced wave equation**): For a monochromatic wave $E = U_0 e^{i\omega t}$, where ω is the **angular frequency** and U_0 is the **complex amplitude**,

$$\nabla^2 U_0 + k^2 U_0 = 0,$$

where k is the optical **wave number**.

If the beam originates at $z = 0$ and the optical field at $z > 0$ remains rotationally symmetric, then $U_0(r, z) = V(r, z)e^{ikz}$, where $r = \sqrt{x^2 + y^2}$ and

$$\frac{1}{r}\frac{\partial}{\partial r}\left(r\frac{\partial V}{\partial r}\right) + \frac{\partial^2 V}{\partial z^2} + 2ik\frac{\partial V}{\partial z} = 0.$$

Paraxial approximation:

$$R = \sqrt{x^2 + y^2 + z^2} = z\sqrt{1 + \frac{x^2 + y^2}{z^2}} \cong z + \frac{x^2 + y^2}{2z}.$$

This assumes the propagation distance for an optical wave is much greater than the transverse spreading of the wave. Thus, we can set $\partial^2 V/\partial z^2 \cong 0$, and obtain the **paraxial wave equation**

$$\frac{1}{r}\frac{\partial}{\partial r}\left(r\frac{\partial V}{\partial r}\right) + 2ik\frac{\partial V}{\partial z} = 0.$$

Plane Wave and Spherical Wave Models

Plane wave: A wave in which the equiphase surfaces (phase fronts) form parallel planes. The description of an infinite plane wave in the plane of the transmitter at $z = 0$ is

$$z = 0: \qquad U_0(x, y, 0) = A_0 e^{i\phi_0},$$

where A_0 is a constant that represents the strength or **amplitude** of the wave field and ϕ_0 is the **phase**.

If the plane wave is propagating along the positive z-axis in free space, the complex amplitude at distance z from the transmitter becomes

$$z > 0: \qquad U_0(x, y, z) = A_0 e^{i\phi_0 + ikz}.$$

Hence, the amplitude remains at A_0 and the plane wave field remains that of a plane wave with changes occurring only in the phase, i.e., $\phi_0 + kz$.

Spherical wave: Characterized by concentric spheres forming the equiphase surfaces. For a spherical wave emanating from the origin, the complex amplitude is given by the limit

$$z = 0: \qquad U_0(x, y, 0) = \lim_{R \to 0} \frac{A_0 e^{ikR}}{4\pi R}.$$

At distance z from the transmitter, the spherical wave under the paraxial approximation is defined by the functional form

$$z > 0: \qquad U_0(x, y, z) = \frac{A_0}{4\pi z} \exp\left[ikz + \frac{ik}{2z}(x^2 + y^2)\right].$$

Therefore the amplitude $A = A_0/4\pi z$ is scaled by distance z.

A plane wave model is used for starlight and other exoatmospheric sources; a spherical wave model is used for a small-aperture source within or near the turbulent atmosphere.

Gaussian-Beam Wave at Transmitter

Gaussian-beam wave TEM_{00}: One of peak amplitude A_0, **spot size radius** W_0 [m], and **phase front radius of curvature** F_0 [m] in the plane of the exit aperture at $z = 0$ is

$$z = 0: \qquad U_0(r, 0) = A_0 \exp\left(-\frac{r^2}{W_0^2}\right) \exp\left(-\frac{ikr^2}{2F_0}\right),$$

where $r = \sqrt{x^2 + y^2}$.

The phase front radius of curvature F_0 identifies a **collimated beam** $F_0 = \infty$, **convergent beam** $F_0 > 0$, or a **divergent beam** $F_0 < 0$.

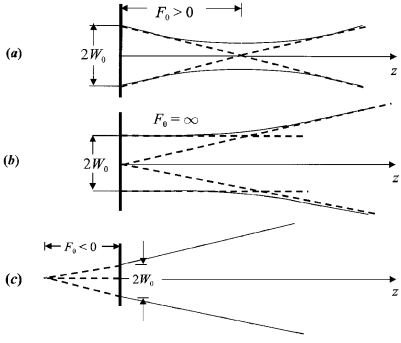

(a) Convergent beam, (b) collimated beam, and (c) divergent beam.

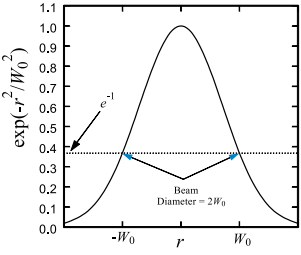

Amplitude profile of a Gaussian-beam wave.

The **beam waist** W_B is defined as the minimum spot size radius of the beam. For a collimated beam, the beam waist is located at the exit aperture of the transmitter ($W_B = W_0$). If the beam is initially convergent, the far-field **divergence angle** is

$$\theta_B = \frac{\lambda}{\pi W_B}, \qquad z \gg \frac{\pi W_B^2}{\lambda}.$$

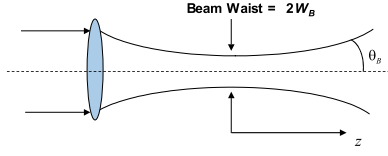

Far-field divergence angle.

Gaussian-Beam Wave at Receiver

Gaussian-beam wave: In the plane of the transmitter $z = 0$, the Gaussian-beam wave with maximum amlitude A_0 at the receiver is

$$z = L: \qquad U_0(\mathbf{r}, L) = \frac{A_0}{\sqrt{\Theta_0^2 + \Lambda_0^2}} \exp\left(-\frac{r^2}{W^2}\right) \times \exp\left(ikL - i\tan^{-1}\frac{\Lambda_0}{\Theta_0} - i\frac{kr^2}{2F}\right).$$

If W_0 and F_0 denote the beam **spot radius** and **phase front radius of curvature** at the transmitter:

- $A = A_0/\sqrt{\Theta_0^2 + \Lambda_0^2}$ is the on-axis **amplitude change** in the beam
- $\Theta_0 = 1 - L/F_0$ describes amplitude change due to **focusing** (refraction)
- $\Lambda_0 = 2L/kW_0^2$ defines amplitude change due to **diffraction**
- $\tan^{-1}(\Lambda_0/\Theta_0)$ is a **longitudinal phase shift**

Beam radius W and radius of curvature F: At the receiver are

$$W = W_0(\Theta_0^2 + \Lambda_0^2)^{1/2}, \qquad F = \frac{F_0(\Theta_0^2 + \Lambda_0^2)(\Theta_0 - 1)}{(\Theta_0^2 + \Lambda_0^2 - \Theta_0)}.$$

Beam waist W_B and **location z_B** are

$$W_B = W_0\sqrt{\frac{\Omega_f^2}{1 + \Omega_f^2}}, \qquad z_B = \frac{F_0}{1 + \Omega_f^2}, \qquad \Omega_f = \frac{2F_0}{kW_0^2}.$$

Hermite-Gaussian Beam Wave

A **higher-order Hermite-Gaussian mode** TEM_{mn} of a collimated beam at the transmitter exit aperture is

$$z = 0: \qquad U_{mn}(x, y, 0) = H_m\left(\frac{\sqrt{2}x}{W_{x,0}}\right) H_n\left(\frac{\sqrt{2}y}{W_{y,0}}\right) \times \exp\left(-\frac{x^2}{W_{x,0}^2} - \frac{y^2}{W_{y,0}^2}\right),$$

where $m, n = 0, 1, 2, \ldots$, the TEM_{00} spot size along the x and y axes at the transmitter is given by $W_{x,0}$ and $W_{y,0}$, respectively; and $H_n(x)$ is the nth Hermite polynomial.

Intensity: At the receiver the **irradiance** is given by

$$\begin{aligned} I_{mn}(x, y, z) &= |U_{mn}(x, y, z)|^2 \\ &= \frac{W_{x,0} W_{y,0}}{W_x W_y} H_m^2\left(\frac{\sqrt{2}x}{W_x}\right) H_n^2\left(\frac{\sqrt{2}y}{W_y}\right) \\ &\quad \times \exp\left(-\frac{x^2}{W_x^2} - \frac{y^2}{W_y^2}\right), \end{aligned}$$

where W_x, W_y denote beam spot sizes of a TEM_{00} beam.

Effective spot radius is given by the rectangular domain $\sigma_{xm}(z) \times \sigma_{yn}(z)$, where

$$\sigma_{x,m}(z) = \sqrt{2m+1}\, W_x(z), \quad m = 0, 1, 2, \ldots,$$
$$\sigma_{y,n}(z) = \sqrt{2n+1}\, W_y(z), \quad n = 0, 1, 2, \ldots.$$

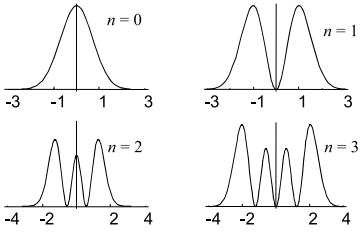

Cross-section view of higher-mode Hermite-Gaussian beams.

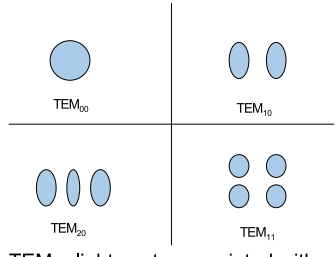

TEM_{mn} light spots associated with some Hermite-Gaussian beams.

Laguerre-Gaussian Beam Wave

A **higher-order Laguerre-Gaussian mode** TEM_{mn} of a collimated beam at the transmitter exit aperture is

$$z = 0:$$
$$U_{mn}(r, \theta, 0) = \left(\frac{\sqrt{2}r}{W_0}\right)^m (-i)^m \exp(im\theta) \times \exp\left(-\frac{r^2}{W_0^2}\right) L_n^{(m)}\left(\frac{2r^2}{W_0^2}\right),$$

where $m, n = 0, 1, 2, \ldots$, W_0 denotes beam spot size of a TEM_{00} beam, and $L_n(x)$ is the nth Laguerre polynomial.

Intensity: At the receiver the **irradiance** is given by

$$z > 0: \qquad I(r, \theta, z) = \frac{W_0^2}{W^2}\left(\frac{2r^2}{W^2}\right)^m \left[L_n^{(m)}\left(\frac{2r^2}{W^2}\right)\right]^2 \exp\left(-\frac{2r^2}{W^2}\right),$$

where W denotes beam spot size of a TEM_{00} beam for $z > 0$.

Effective spot radius: For a Laguerre-Gaussian beam is given by

$$\sigma_{mn}(z) = \sqrt{2n + m + 1}\, W(z); \quad m, n = 0, 1, 2, \ldots.$$

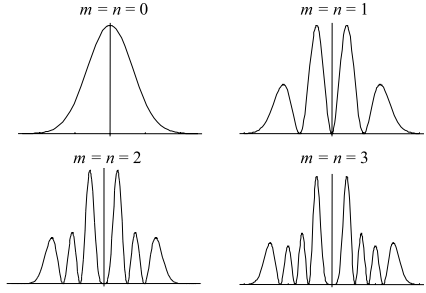

Cross-section view of higher-mode Laguerre-Gaussian beams.

Example

Assume the following beam characteristics of a unit amplitude ($A_0 = 1$) Gaussian-beam wave TEM_{00} at the transmitter:

$$W_0 = 0.03 \text{ m}, \qquad F_0 = 500 \text{ m}, \qquad \lambda = 0.633 \ \mu\text{m}.$$

For a receiver at distance $z = L = 1200$ m from the transmitter, calculate the following beam characteristics:
(a) spot radius at the receiver,
(b) radius of curvature at the receiver,
(c) on-axis irradiance at the receiver,
(d) propagation distance to beam waist,
(e) beam radius at the waist,
(f) beam radius at the geometric focus.

Solution: First calculate the beam parameters:

$$\Theta_0 = 1 - \frac{L}{F_0} = -1.4, \qquad \Lambda_0 = \frac{2L}{kW_0^2} = 0.2687$$

(a) $W = W_0\sqrt{\Theta_0^2 + \Lambda_0^2} = 4.3$ cm

(b) $F = \dfrac{F_0(\Theta_0^2 + \Lambda_0^2)(\Theta_0 - 1)}{(\Theta_0^2 + \Lambda_0^2 - \Theta_0)} = -710.5$ m

(c) $I(0, L) = W_0^2/W^2 = 0.492$

(d) $z_B = \dfrac{F_0}{1 + \Omega_f^2} = 494$ m

(e) $W_B = W_0\sqrt{\dfrac{\Omega_f^2}{1 + \Omega_f^2}} = 0.33$ cm

(f) $W_f = 2F_0/kW_0^2 = 0.34$ cm

Atmospheric Propagation: Second-Order Statistics

An optical wave propagating through the atmosphere experiences a variety of deleterious effects relevant to optical communication systems, laser radar, and imaging. Amplitude or irradiance fluctuations are important in direct detection systems, whereas phase fluctuations are often more significant in (coherent) homodyne or heterodyne detection systems.

Common atmospheric effects on propagating optical waves include the following:

- **Beam spreading**—beam divergence beyond pure diffraction causing a power reduction at the receiver
- **Beam wander** (or **steering**)—angular deviation of the beam from the line-of-sight path, possibly causing the beam to miss the receiver
- **Image dancing**—fluctuations in the beam angle-of-arrival, causing the focus to move ("dance") in the image plane
- **Beam scintillation**—irradiance fluctuations within the beam cross section, causing loss of signal-to-noise ratio and inducing deep random fades
- **Loss of spatial coherence**—limits the effective aperture diameter in an imaging system and in a coherent detector.

Except for beam scintillation, the others are directly related to a second-order field moment known as the **mutual coherence function** MCF.

Rytov Approximation

Neglecting polarization effects, a monochromatic optical wave propagating through a random medium is governed by the **stochastic Helmholtz equation**

$$\nabla^2 U + k^2 n^2(\mathbf{R}) U = 0.$$

Under **weak irradiance fluctuations** $\sigma_1^2 = 1.23 C_n^2 k^{7/6} L^{11/6} < 1$ solutions can be analyzed by the classical Rytov approximation.

Rytov method: The optical field at propagation distance L is

$$\begin{aligned} U(\mathbf{r}, L) &= U_0(\mathbf{r}, L) \exp[\psi(\mathbf{r}, L)] \\ &= U_0(\mathbf{r}, L) \exp[\psi_1(\mathbf{r}, L) + \psi_2(\mathbf{r}, L) + \cdots], \end{aligned}$$

where $U_0(\mathbf{r}, L)$ is the free-space wave at $z = L$ and $\psi_1(\mathbf{r}, L)$ and $\psi_2(\mathbf{r}, L)$ are first-order and second-order **complex phase perturbations**.

Mean field—coherent part of the field

$$\begin{aligned} \langle U(\mathbf{r}, L) \rangle &= U_0(\mathbf{r}, L) \langle \exp[\psi(\mathbf{r}, L)] \rangle \\ &= U_0(\mathbf{r}, L) \exp\left[-2\pi^2 k^2 L \int_0^\infty \kappa \Phi_n(\kappa) d\kappa \right] \end{aligned}$$

Mutual coherence function MCF—correlation function of the field

$$\begin{aligned} \Gamma_2(\mathbf{r}_1, \mathbf{r}_2, L) &= \langle U(\mathbf{r}_1, L) U^*(\mathbf{r}_2, L) \rangle \\ &= U_0(\mathbf{r}_1, L) U_0^*(\mathbf{r}_2, L) \\ &\quad \times \langle \exp[\psi(\mathbf{r}_1, L) + \psi^*(\mathbf{r}_2, L)] \rangle \\ &= U_0(\mathbf{r}_1, L) U_0^*(\mathbf{r}_2, L) \\ &\quad \times \exp\left[-4\pi^2 k^2 L \int_0^1 \int_0^\infty \kappa \Phi_n(\kappa) \right. \\ &\quad \times \left\{ 1 - \exp\left(-\frac{\Lambda L \kappa^2 \xi^2}{k} \right) \right. \\ &\quad \left. \left. \times J_0[|(1 - \overline{\Theta}\xi)\mathbf{p} - 2i\Lambda\xi\mathbf{r}|\kappa] \right\} d\kappa d\xi \right], \end{aligned}$$

where $\mathbf{p} = \mathbf{r}_1 - \mathbf{r}_2$ and $\mathbf{r} = \frac{1}{2}(\mathbf{r}_1 + \mathbf{r}_2)$.

Extended Huygens-Fresnel Principle

Extended Huygens-Fresnel Principle: Expresses the field of the optical wave at $z = L$ as

$$U(\mathbf{r}, L) = -\frac{ik}{2\pi L}\exp(ikL)\iint_{-\infty}^{\infty} d^2 s U_0(\mathbf{s}, 0) \times \exp\left[\frac{ik|\mathbf{s}-\mathbf{r}|^2}{2L} + \psi(\mathbf{r}, \mathbf{s})\right],$$

where $U_0(\mathrm{s}, 0)$ is the optical wave at the transmitter. Here, $\psi(\mathbf{r}, \mathbf{s})$ is the random part of the **complex phase of a spherical wave** propagating in the turbulent medium from the point $(\mathbf{s}, 0)$ to the point $(\mathbf{r}, L)$.

This principle is known to be applicable only through first-order and second-order field moments, but under all conditions of irradiance fluctuations (i.e., both weak and strong).

Mean field—leads to the expression

$$\langle U(\mathbf{r}, L)\rangle = U_0(\mathbf{r}, L)\exp\left[-2\pi^2 k^2 L\int_0^{\infty} \kappa\Phi_n(\kappa)d\kappa\right],$$

which is the same as obtained by the Rytov method.

Mutual coherence function MCF—the field correlation function leads to the expression

$$\Gamma_2(\mathbf{r}_1, \mathbf{r}_2, L) = \langle U(\mathbf{r}_1, L)U^*(\mathbf{r}_2, L)\rangle = \frac{W_0^2}{8\pi}\iint_{-\infty}^{\infty} d^2 u \exp\left\{-\frac{\rho^2}{2W_0^2} - \frac{1}{8}W^2 u^2 + \frac{\overline{\Theta}}{2\Lambda}\mathbf{u}\cdot\mathbf{p} + i\mathbf{u}\cdot\mathbf{r} - \frac{1}{2}D_{\mathbf{sp}}[\mathbf{p}, \mathbf{p} - (L/k)\mathbf{u}]\right\},$$

where

$$D_{\mathbf{sp}}[\mathbf{p}, \mathbf{p} - (L/k)\mathbf{u}] = 8\pi^2 k^2 L\int_0^1\int_0^{\infty} \kappa\Phi_n(\kappa)\{1 - J_0[|\mathbf{p} - (L/k)\mathbf{u}|\kappa]\}d\kappa d\xi.$$

For plane waves and spherical waves, the MCF is the same as found by the Rytov approximation, but not in the Gaussian-beam wave case.

Parabolic Equation Method

Parabolic Equation Method: Based on solving a parabolic equation for each moment of the field.

Mean field—the coherent field $\langle U(\mathbf{r},z)\rangle$ at propagation distance z is a solution of

$$2ik\frac{\partial\langle U(\mathbf{r},z)\rangle}{\partial z}+\nabla_T^2\langle U(\mathbf{r},z)\rangle+2k^2\langle n_1(\mathbf{r},z)U(\mathbf{r},z)\rangle=0,$$

where $\nabla_T^2=\partial^2/\partial x^2+\partial^2/\partial y^2$ denotes the transverse Laplacian operator. Solving this equation yields

$$\langle U(\mathbf{r},L)\rangle=U_0(\mathbf{r},L)\exp\left[-2\pi^2k^2L\int_0^\infty \kappa\Phi_n(\kappa)d\kappa\right],$$

which is the same expression as obtained by the Rytov method.

Mutual coherence function—$\Gamma_2(\mathbf{r}_1,\mathbf{r}_2,z)=\langle U(\mathbf{r}_1,z)U^*(\mathbf{r}_2,z)\rangle$ at propagation distance z satisfies

$$\begin{aligned}&2ik\frac{\partial}{\partial z}\Gamma_2(\mathbf{r}_1,\mathbf{r}_2,z)\\&\quad+(\nabla_{T1}^2-\nabla_{T2}^2)\Gamma_2(\mathbf{r}_1,\mathbf{r}_2,z)\\&\quad+2k^2\langle[n_1(\mathbf{r}_1,z)-n_1(\mathbf{r}_2,z)]U(\mathbf{r}_1,z)U^*(\mathbf{r}_2,z)\rangle=0.\end{aligned}$$

The solution of this equation for an infinite plane wave leads to

$$\Gamma_2(\mathbf{r}_1,\mathbf{r}_2,z)=\exp\left\{-4\pi^2k^2z\int_0^\infty \kappa\Phi_n(\kappa)[1-J_0(\kappa\rho)]d\kappa\right\},$$

which is the same as that derived from the Rytov approximation. The same is true for a spherical wave but not in the case of a Gaussian-beam wave.

The parabolic equation method is valid under all conditions of irradiance fluctuations. Moreover, it is considered more fundamental than the extended Huygens principle and is therefore the method most often used to calculate the fourth-order field moment.

Mean Irradiance and Beam Spreading

Beam spreading in a vacuum is a consequence of diffraction. In the presence of atmospheric turbulence there is additional beam spreading, producing a larger **beam spot size** than diffraction alone. In both cases, the resulting beam spot size determines the mean irradiance.

Irradiance in free space: At propagation distance L from the transmitter of a unit-amplitude Gaussian-beam wave with initial beam radius W_0, is given by

$$I(r,L) = \frac{W_0^2}{W^2} e^{-2r^2/W^2}.$$

- $W = W_0\sqrt{(1-L/F_0)^2 + (2L/kW_0^2)^2}$: (beam radius at $z=L$)
- F_0: (phase front radius of curvature at transmitter)
- k: (optical wave number $= 2\pi/\lambda$)
- $r = \sqrt{x^2+y^2}$: (transverse distance from optical axis)

Mean irradiance in turbulence: In the presence of atmospheric turbulence, the **mean irradiance profile** (over a long time average) can usually still be approximated by a Gaussian function, i.e.,

$$\langle I(r,L)\rangle = \Gamma_2(\mathbf{r},\mathbf{r},L) \cong \frac{W_0^2}{W_e^2} e^{-2r^2/W_e^2},$$

where W_e is the "effective" **long-time-average** beam radius given by

$$W_e = W\sqrt{1 + 1.63\sigma_1^{12/5}\Lambda}, \quad 0 \le \sigma_1^2 < \infty.$$

The parameters appearing above in the effective beam radius are defined by

$$\sigma_1^2 = 1.23 C_n^2 k^{7/6} L^{11/6}, \quad \Lambda = \frac{2L}{kW^2}.$$

Beam Wander

Beam wander (or **beam steering**): Random deflections a finite beam will experience as it propagates.

As a result of large scales in the atmosphere, the centroid of the "short-term beam spot size" will wander randomly in the plane of a receiver aperture. But, the actual path of the beam is more like that of a corkscrew rather than a "moving wand."

Beam wander can be statistically characterized by the variance of the beam displacement along an axis or by the variance of the magnitude of the beam displacement. It has a time constant on the order of:

$$\tau = \frac{\text{beam size}}{\text{wind speed}}.$$

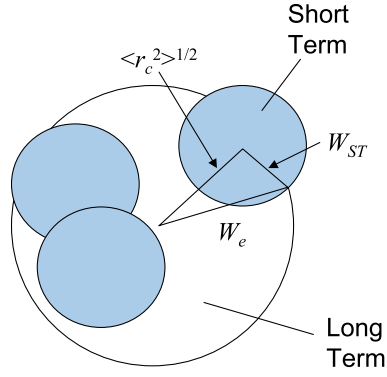

The shaded circles represent the short-term beam size W_{ST} and the large circle is the long-term beam size W_e.

Because beam wander is caused mostly by large-scale turbulence, diffraction effects are negligible whenever the receiver aperture diameter D is greater than the size of the Fresnel zone $\sqrt{L/k}$.

In isotropic turbulence, the variances along the x- and y-axes are equal and the variance of the magnitude is twice the single axis variance. The rms (root-mean-square) centroid **displacement** is $\langle \beta_c^2 \rangle^{1/2} = 0.75 \langle r_c^2 \rangle^{1/2}$, where

$$\langle r_c^2 \rangle^{1/2} = \sqrt{W_e^2 - W_{ST}^2} = \sqrt{2.42 C_n^2 L^3 W_0^{-1/3}}.$$

Spatial Coherence Radius: Plane Wave

Temporal coherence: The ability of a light beam to interfere with a delayed version of itself. However, in atmospheric propagation it is usually the spatial coherence that is of greater importance.

Spatial coherence: The ability of a light beam to interfere with a spatially shifted version of itself.

Mutual coherence function MCF for an infinite plane wave that has propagated a distance L is given by

$$\Gamma_2(\rho, L) = \exp\left[-\frac{1}{2}D(\rho, L)\right],$$

where $\rho = |\mathbf{r}_1 - \mathbf{r}_2|$ is the separation distance between two points on the phase front and $D(\rho, L)$ is the **wave structure function** WSF

$$D(\rho, L) = 2.91k^2\rho^{5/3}\int_0^L C_n^2(z)dz, \quad l_0 \ll \rho_0 \ll L_0.$$

The WSF is composed of two parts: $D(\rho, L) = D_\chi(\rho, L) + D_S(\rho, L)$, where $D_\chi(\rho, L)$ is the **log-amplitude structure function** and $D_S(\rho, L)$ is the **phase structure function**.

> Because the WSF is dominated by phase fluctuations rather than amplitude fluctuations, the phase structure function and WSF are often considered essentially the same.

Plane wave coherence radius ρ_0: Defined as that separation distance at which the normalized MCF reduces to $1/e$. Thus,

$$\rho_0 \equiv \rho_{\text{pl}} = \begin{cases} \left[1.46k^2\int_0^L C_n^2(z)dz\right]^{-3/5}, & l_0 \ll \rho_0 \ll L_0, \\ (1.46C_n^2k^2L)^{-3/5}, & l_0 \ll \rho_0 \ll L_0, \quad C_n^2 = \text{const.} \end{cases}$$

Spatial Coherence Radius: Spherical Wave

Mutual coherence function MCF for a spherical wave that has propagated a distance L leads to

$$\Gamma_2(\mathbf{p}, \mathbf{r}, L) = \frac{1}{(4\pi L)^2} \exp\left[\frac{ik}{L}\mathbf{p}\cdot\mathbf{r} - \frac{1}{2}D(\rho, L)\right],$$

where $\mathbf{p} = \mathbf{r}_1 - \mathbf{r}_2$, $\mathbf{r} = \frac{1}{2}(\mathbf{r}_1 + \mathbf{r}_2)$, and $\rho = |\mathbf{r}_1 - \mathbf{r}_2|$ is the separation distance between two points on the phase front.

The quantity $D(\rho, L)$ is the **wave structure function** WSF

$$D(\rho, L) = 2.91k^2\rho^{5/3}\int_0^L C_n^2(z)(z/L)^{5/3}dz, \quad l_0 \ll \rho_0 \ll L_0,$$

which, for constant C_n^2, becomes

$$D(\rho, L) = 1.09C_n^2k^2L\rho^{5/3}, \quad l_0 \ll \rho_0 \ll L_0.$$

Spherical wave coherence radius: Defined as that separation distance at which the modulus of the exponential function in the MCF reduces to $1/e$. Therefore,

$$\rho_0 \equiv \rho_{\text{sph}} = \begin{cases} \left[1.46k^2\displaystyle\int_0^L C_n^2(z)(z/L)^{5/3}dz\right]^{-3/5}, \\ \quad l_0 \ll \rho_0 \ll L_0, \\ (0.55C_n^2k^2L)^{-3/5}, \quad l_0 \ll \rho_0 \ll L_0, \quad C_n^2 = \text{const.} \end{cases}$$

The above expressions for the spatial coherence radius of an infinite plane wave (previous page) and a point source (spherical wave) can be derived by geometrical optics and are generally considered valid under all conditions of irradiance fluctuations.

Spatial Coherence Radius: Gaussian-Beam Wave

The **mutual coherence function** MCF is a function of only the scalar distance $\rho = |\mathbf{r}_1 - \mathbf{r}_2|$ for an unbounded wave or when $\mathbf{r}_1 = -\mathbf{r}_2$.

MCF: For a collimated Gaussian-beam wave that has propagated a distance L for points $\mathbf{r}_1 = -\mathbf{r}_2$ (and $l_0 \ll \rho \ll L_0$) becomes

$$\Gamma_2(\rho, L) = \frac{W_0^2}{W^2} \exp\left[-1.13(q\Lambda)^{5/6} - \frac{\Lambda}{4}\left(\frac{k\rho^2}{L}\right) - \frac{3a}{8}\left(\frac{qk\rho^2}{L}\right)^{5/6}\right].$$

Here, $\Lambda = 2L/kW^2$, $q = 1.56(C_n^2 k^{7/6} L^{11/6})^{6/5}$ is a strength of turbulence parameter, and parameter a is defined by

$$a = \frac{1 - \Theta^{8/3}}{1 - \Theta}, \qquad \Theta \geq 0.$$

The refractive beam parameter Θ is defined by $\Theta = 1/[1 + (2L/kW_0^2)^2]$.

Modulus of the complex degree of coherence: The loss of spatial coherence can be deduced from the e^{-1} value of the DOC:

$$\mathrm{DOC}(\mathbf{r}_1, \mathbf{r}_2, L) = \frac{\Gamma_2(\mathbf{r}_1, \mathbf{r}_2, L)}{\sqrt{\Gamma_2(\mathbf{r}_1, \mathbf{r}_1, L)\Gamma_2(\mathbf{r}_2, \mathbf{r}_2, L)}} = \exp\left[-\frac{1}{2}D(\mathbf{r}_1, \mathbf{r}_2, L)\right],$$

where $D(\mathbf{r}_1, \mathbf{r}_2, L)$ is the **wave structure function** (WSF).

Spatial coherence radius: For constant C_n^2, approximated by (under weak irradiance fluctuations)

$$\rho_0 = [0.55C_n^2 k^2 L(a + 0.62\Lambda^{11/6})]^{-3/5}, \quad l_0 \ll \rho_0 \ll L_0.$$

The spatial coherence radius always lies between that of an infinite plane wave (for large beams) and a spherical wave (for small beams) under weak irradiance fluctuations.

Fried's Parameter and the Phase Structure Function

A parameter that is often used in place of the spatial coherence radius is the related **Fried's parameter** r_0,

$$r_0 = 2.1\rho_0.$$

Also called the atmospheric coherence width, r_0 describes the largest effective telescope diameter for image resolution, and is also an upper bound for aperture diameter in maximizing the normalized signal-to-noise ratio SNR in a coherent detection system.

For irradiance (or amplitude) fluctuations, the important scale sizes are on the order of the Fresnel zone $\sqrt{L/k}$, but for **phase fluctuations** it is the larger scales that are influential. Phase fluctuations are particularly important in homodyne or heterodyne detection systems.

The **phase structure function** at propagation distance L is defined by

$$D_S(\rho, L) = \left\langle (S_1 - S_2)^2 \right\rangle,$$

where S_1 and S_2 denote phase measurements at two points on the phase front separated by distance ρ.

Plane wave—for an infinite plane wave, the phase structure function is given by ($C_n^2 = \text{constant}$)

$$D_S(\rho, L) = \begin{cases} 1.64 C_n^2 k^2 L l_0^{-1/3} \left[1 + 0.64 (k l_0^2 / L)^{1/6}\right] \rho^2, & \rho \ll l_0, \\ 1.46 C_n^2 k^2 L \rho^{5/3}, & l_0 \ll \rho \ll \sqrt{L/k}, \\ 2.91 C_n^2 k^2 L \rho^{5/3}, & \sqrt{L/k} \ll \rho \ll L_0. \end{cases}$$

Angle-of-Arrival and Image Jitter

Angle-of-arrival: A measure of the instantaneous direction of propagation of an optical wave upon arrival at a receiver—the angle between the actual plane of the phase front at the receiver and some plane of reference.

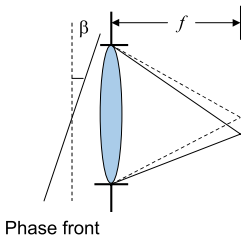

Angle-of-arrival and image jitter.

If ΔS denotes the total phase shift across a collecting lens of diameter D and Δl the corresponding optical path difference, then

$$k\Delta l = \Delta S.$$

If we assume that β is small so that $\sin\beta \cong \beta$, the angle-of-arrival is defined by

$$\beta = \frac{\Delta l}{D} = \frac{\Delta S}{kD}. \qquad \text{[radian]}$$

Further assuming $\langle\beta\rangle = 0$, we deduce the **variance of the angle-of-arrival** (for an infinite plane wave)

$$\langle\beta^2\rangle = \frac{\langle(\Delta S)^2\rangle}{(kD)^2} = \frac{D_S(D,L)}{(kD)^2} = 2.91D^{-1/3}\int_0^L C_n^2(z)dz,$$

$$D \gg l_0.$$

where $D_S(\rho, L)$ is the phase structure function and l_0 is inner scale.

Image jitter (dancing): Produced by angle-of-arrival fluctuations of an optical wave in the plane of the receiver aperture in the focal plane of an imaging system.

The **rms image displacement** is the root-mean-square (rms) angle-of-arrival $\langle\beta^2\rangle^{1/2}$ multiplied by f, where f is the focal length of the receiver collecting lens.

Example

A collimated beam is propagated through atmospheric turbulence to a receiver located 1 km from the transmitter. Given that the beam radius at the transmitter is 1 cm, the wavelength is 1.55 μm, and $C_n^2 = 10^{-13}$ m$^{-2/3}$, calculate

(a) the spot size W in free space at the receiver,
(b) the spot size W_e in turbulence at the receiver,
(c) the rms displacement $\langle r_c^2 \rangle^{1/2}$, and
(d) the short term beam radius W_{ST} at the receiver.

Solution: First calculate the parameters

$$\Theta_0 = 1 - \frac{L}{F_0} = 1, \qquad \Lambda_0 = \frac{2L}{kW_0^2} = 4.934$$

$$\Theta = \frac{\Theta_0}{\Theta_0^2 + \Lambda_0^2} = 0.0395, \qquad \Lambda = \frac{\Lambda_0}{\Theta_0^2 + \Lambda_0^2} = 0.1947$$

$$\sigma_1^2 = 1.23 C_n^2 k^{7/6} L^{11/6} = 1.99$$

(a) $W = \sqrt{\Theta_0^2 + \Lambda_0^2} = 5$ cm

(b) $W_e = W\sqrt{1 + 1.63\sigma_1^{12/5}\Lambda} = 6.6$ cm

(c) $\langle r_c^2 \rangle^{1/2} = \sqrt{2.42 C_n^2 L^3 W_0^{-1/3}} = 3.35$ cm

(d) $W_{ST} = \sqrt{W_e^2 - \langle r_c^2 \rangle^{1/2}} = 5.7$ cm

Example

A collimated beam is propagated through atmospheric turbulence to a receiver located 450 meters from the transmitter. Given that the beam radius at the transmitter is 0.5 cm, the wavelength is 0.5 μm, and $C_n^2 = 0.5 \times 10^{-13}$ m$^{-2/3}$, calculate

(a) the free-space (no turbulence) spot diameter at the receiver.
(b) the spot size diameter of the beam in turbulence at the receiver.
(c) the spatial coherence radius ρ_0 and Fried's parameter r_0 at the receiver.

Solution: To begin, first make the calculations:

$$\Lambda_0 = \frac{2L}{kW_0^2} = 2.865, \qquad \Lambda = \frac{\Lambda_0}{1+\Lambda_0^2} = 0.311$$

$$a = \frac{(1-\Theta^{8/3})}{1-\Theta} = 1.119, \qquad \sigma_1^2 = 1.23 C_n^2 k^{7/6} L^{11/6} = 0.862$$

(a) $2W = 2W_0\sqrt{1+\Lambda_0^2} = 3.034$ cm

(b) $2W_e = 2W\sqrt{1+1.625\sigma_1^{12/5}\Lambda} = 3.620$ cm

(c) $\rho_0 = \left[0.55 C_n^2 k^2 L (a + 0.62\Lambda^{11/6})\right]^{-3/5} = 0.96$ cm
$r_0 = 2.1\rho_0 = 2.02$ cm

Atmospheric Propagation: Fourth-Order Statistics

Irradiance (or intensity) fluctuations known as **scintillation** can be deduced from knowledge of the general fourth-order field moment of an optical wave. In the context of Rytov theory, many early investigations into the statistical characteristics of an optical wave propagating through atmospheric turbulence were concerned with the **log-amplitude variance** or **log-irradiance variance**.

The general fourth-order moment is also required to generate the **irradiance covariance function**. Combined with **Taylor's frozen turbulence hypothesis**, the **temporal covariance function** can be deduced from the spatial covariance function. By application of the Fourier transform to the temporal covariance function, the **power spectrum** of irradiance fluctuations can then be found.

The **scintillation index** (or normalized variance of intensity) is important in that it is used in predicting signal fades and bit error rates. Namely, stronger scintillation generally yields a larger probability of fade. The **correlation width** describes the average speckle size in the pupil plane of the receiver. If the receiver aperture is larger than the correlation width, some **aperture averaging** is likely to occur. On the other hand, the receiver acts like a "point receiver" when its aperture size is comparable to or smaller than the correlation width of intensity fluctuations.

Rytov Approximation: Fourth-Order Specializations

The fourth-order coherence function can be exploited to obtain useful statistics concerning the irradiance of the optical wave.

Fourth-order coherence function: Under the **Rytov method**, it is is defined by

$$\begin{aligned}\Gamma_4(\mathbf{r}_1,\mathbf{r}_2,\mathbf{r}_3,\mathbf{r}_4 L) &= \left\langle U(\mathbf{r}_1,L)U^*(\mathbf{r}_2,L)U(\mathbf{r}_3,L)U^*(\mathbf{r}_4,L)\right\rangle \\ &= U_0(\mathbf{r}_1,L)U_0^*(\mathbf{r}_2,L)U_0(\mathbf{r}_3,L)U_0^*(\mathbf{r}_4,L) \\ &\quad \times\left\langle \exp[\psi(\mathbf{r}_1,L)+\psi^*(\mathbf{r}_2,L)+\psi(\mathbf{r}_3,L) \right. \\ &\quad \left. +\psi^*(\mathbf{r}_4,L)]\right\rangle.\end{aligned}$$

Second moment of the irradiance—by specifying $\mathbf{r}_1 = \mathbf{r}_2 = \mathbf{r}_3 = \mathbf{r}_4 = \mathbf{r}$, the fourth-order coherence function reduces to

$$\left\langle I^2(\mathbf{r},L)\right\rangle = \Gamma_4(\mathbf{r},\mathbf{r},\mathbf{r},\mathbf{r},L).$$

Covariance function of irradiance—a two-point specialization of the general fourth-order moment defined by the normalized quantity

$$B_I(\mathbf{r}_1,\mathbf{r}_2,L) = \frac{\Gamma_4(\mathbf{r}_1,\mathbf{r}_1,\mathbf{r}_2,\mathbf{r}_2,L)}{\Gamma_2(\mathbf{r}_1,\mathbf{r}_1,L)\Gamma_2(\mathbf{r}_2,\mathbf{r}_2,L)} - 1.$$

Scintillation index—in the special case $\mathbf{r}_1 = \mathbf{r}_2 = \mathbf{r}$, the covariance function reduces to

$$\sigma_I^2(\mathbf{r},L) = B_I(\mathbf{r},\mathbf{r},L) = \frac{\langle I^2(\mathbf{r},L)\rangle}{\langle I(\mathbf{r},L)\rangle^2} - 1.$$

Scintillation Index: Theory

Scintillation: Refers to the temporal or spatial fluctuations in the irradiance of an optical wave (e.g., star twinkle) caused by small random index-of-refraction fluctuations.

Scintillation index: The variance of irradiance fluctuations scaled by the square of the mean irradiance.

- The scintillation index increases with increasing values of the **Rytov variance** $\sigma_1^2 = 1.23 C_n^2 k^{7/6} L^{11/6}$ until it reaches a maximum value greater than unity (possibly up to 5 or 6) in the regime characterized by random focusing by the large refractive inhomogeneities (eddies). Here, C_n^2 is the refractive index structure constant, $k = 2\pi/\lambda$ is optical wave number, and L is propagation path length.
- With increasing path length, the focusing effect is weakened by multiple scattering and the fluctuations slowly begin to decrease, saturating at a level approaching unity from above.
- Qualitatively, saturation occurs because multiple scattering causes the optical wave to become increasingly less coherent spatially as it propagates.

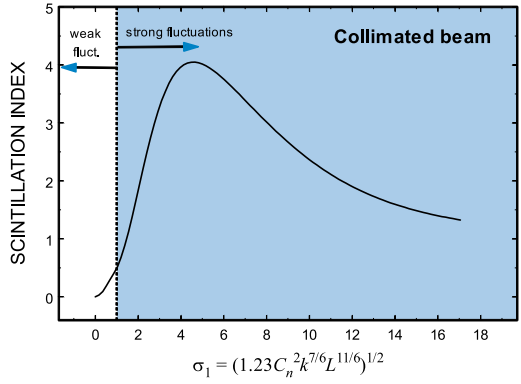

Scintillation Index: Plane Wave

Weak fluctuations—under the Rytov approximation, the **scintillation index** for an infinite plane wave propagating along a horizontal path is given by the **Rytov variance** ($l_0 = 0, L_0 = \infty$)

$$\sigma_I^2 = \sigma_1^2 = 1.23 C_n^2 k^{7/6} L^{11/6}, \quad \sigma_1^2 < 1.$$

Strong fluctuations—under strong (or weak) irradiance fluctuation conditions, the Rytov variance is a measure of turbulence strength and the **scintillation index** is described by ($l_0 = 0, L_0 = \infty$)

$$\sigma_I^2 = \exp\left[\frac{0.49\sigma_1^2}{(1+1.11\sigma_1^{12/5})^{7/6}} + \frac{0.51\sigma_1^2}{(1+0.69\sigma_1^{12/5})^{5/6}}\right] - 1,$$

$$0 \le \sigma_1^2 < \infty.$$

Downlink path—the scintillation index is the same as directly above, provided we define the Rytov variance by

$$\sigma_1^2 = 2.25 k^{7/6} (H - h_0)^{5/6} \sec^{11/6}(\zeta) \int_{h_0}^{H} C_n^2(h) \left(\frac{h - h_0}{H - h_0}\right)^{5/6} dh,$$

where h is altitude, h_0 is height of receiver, H is height of satellite, and ζ is the zenith angle.

A finite outer scale has little effect in the regime $\sigma_1 < 1$, but will tend to reduce scintillation in the regime $\sigma_1 > 4$.

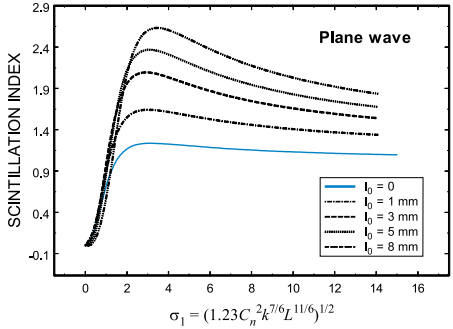

Scintillation Index: Spherical Wave

Weak fluctuations—under the Rytov approximation, the **scintillation index** for a spherical plane wave propagating along a horizontal path is given by the (spherical wave) **Rytov variance** ($l_0 = 0, L_0 = \infty$)

$$\sigma_I^2 = \beta_0^2 = 0.5 C_n^2 k^{7/6} L^{11/6}, \quad \beta_0^2 < 1.$$

Strong fluctuations—under general irradiance fluctuation conditions, the Rytov variance is a measure of turbulence strength and the **scintillation index** is described by ($l_0 = 0, L_0 = \infty$)

$$\sigma_I^2 = \exp\left[\frac{0.49\beta_0^2}{(1+0.56\beta_0^{12/5})^{7/6}} + \frac{0.51\beta_0^2}{(1+0.69\beta_0^{12/5})^{5/6}}\right] - 1,$$

$$0 \le \beta_0^2 < \infty.$$

Uplink path—for uplink paths the scintillation index is the same as directly above provided we "redefine" the Rytov variance by

$$\beta_0^2 = 2.25 k^{7/6} (H - h_0)^{5/6} \sec^{11/6}(\zeta) \int_{h_0}^{H} C_n^2(h) \left(\frac{h - h_0}{H - h_0}\right)^{5/6} dh.$$

The scintillation index of an uplink spherical wave (under weak fluctuations) is the same as a downlink plane wave.

A finite outer scale has little effect in the regime $\beta_0 < 1$, but will tend to reduce scintillation in the regime $\beta_0 > 4$.

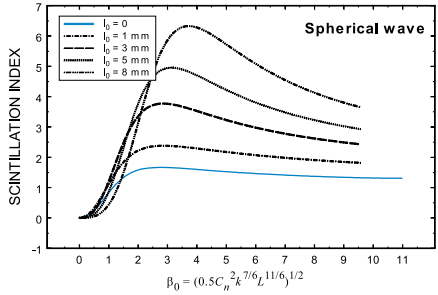

Scintillation Index: Gaussian-Beam Wave

Weak fluctuations—under the Rytov approximation, the **scintillation index** for a Gaussian-beam wave propagating along a horizontal path is given by ($l_0 = 0$, $L_0 = \infty$)

$$\sigma_I^2(r, L) = 2.65\sigma_1^2 \Lambda^{5/6}\left[1 - {}_1F_1(-5/6;\, 1;\, 2r^2/W^2)\right] + \sigma_B^2,$$

where σ_B^2 is the longitudinal (on-axis) component given by

$$\sigma_B^2 = 3.86\sigma_1^2 \mathrm{Re}\left[i^{5/6}\, {}_2F_1\left(-\frac{5}{6}, \frac{11}{6}; \frac{17}{6}; \overline{\Theta} + i\Lambda\right) - \frac{11}{16}\Lambda^{5/6}\right].$$

Here, ${}_1F_1$ and ${}_2F_1$ are hypergeometric-type functions.

Strong fluctuations—under strong (or weak) irradiance fluctuation conditions, the **scintillation index** is approximated by ($l_0 = 0$, $L_0 = \infty$)

$$\sigma_I^2(r, L) = 4.42\sigma_1^2 \left(\frac{\Lambda}{1 + 1.63\sigma_1^{12/5}\Lambda}\right) \frac{r^2}{W^2(1 + 1.63\sigma_1^{12/5}\Lambda)}$$
$$+ \exp\left[\frac{0.49\sigma_B^2}{(1 + 0.56(1 + \Theta)\sigma_B^{12/5})^{7/6}} + \frac{0.51\sigma_B^2}{(1 + 0.69\sigma_B^{12/5})^{5/6}}\right] - 1,$$

$$0 \le \sigma_1^2 < \infty.$$

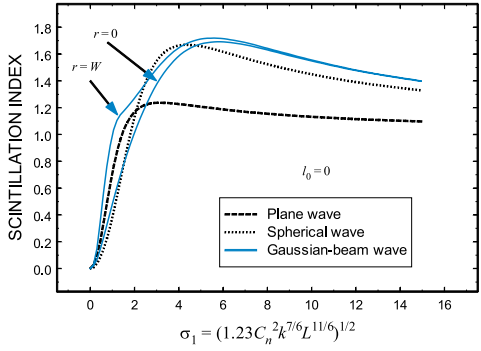

The solid curves depict on-axis ($r = 0$) and off-axis ($r = W$) scintillation of a beam wave.

Covariance Function: Plane Wave

Weak fluctuations—under the Rytov approximation, the **covariance function** for a plane wave propagating along a horizontal path is given by ($l_0 = 0$, $L_0 = \infty$)

$$B_I(\rho) \cong \sigma_1^2\left[1 - 2.37\left(\frac{k\rho^2}{L}\right)^{5/6} + 1.92\left(\frac{k\rho^2}{L}\right) + \cdots\right],$$

$$l_0 \ll \rho \ll \sqrt{L/k}.$$

Strong fluctuations—under strong (or weak) irradiance fluctuation conditions, the **covariance function** is described by ($l_0 = 0$, $L_0 = \infty$)

$$B_I(\rho) = \exp\left[\frac{0.49\sigma_1^2}{(1 + 1.11\sigma_1^{12/5})^{7/6}}\,{}_1F_1\left(\frac{7}{6}; 1; -\frac{k\rho^2\eta_x}{4L}\right)\right.$$

$$\left. + \frac{0.50\sigma_1^2}{(1 + 0.69\sigma_1^{12/5})^{5/6}}\left(\frac{k\rho^2\eta_y}{L}\right)^{5/12} K_{5/6}\left(\sqrt{\frac{k\rho^2\eta_y}{L}}\right)\right] - 1,$$

where $K_\nu(x)$ is a modified Bessel function, $\eta_x = 2.61/(1 + 1.11\sigma_1^{12/5})$, and $\eta_y = 3(1 + 0.69\sigma_1^{12/5})$.

Correlation width of the irradiance ρ_c: zero crossing (or $1/e^2$) point of $b_I(\rho) = B_I(\rho)/B_I(0)$:

$$\rho_c = \begin{cases} \sqrt{L/k}, & \sigma_1^2 < 1 \\ \rho_0, & \sigma_1^2 \gg 1. \end{cases}$$

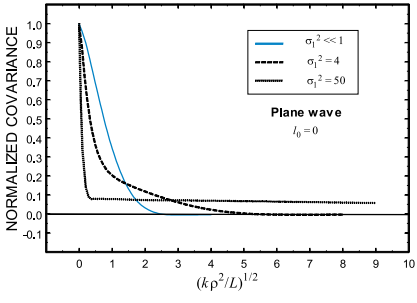

Normalized covariance $b_I(\rho) = B_I(\rho)/B_I(0)$.

The long correlation tail for strong fluctuations is characterized by the **scattering disk** $L/k\rho_0$.

Temporal Power Spectrum: Plane Wave

Taylor frozen turbulence hypothesis—spatial statistics can be converted to temporal statistics by knowledge of the average transverse wind speed V. Hence, we assume that the turbulent eddies are "frozen" over short periods as they are blown past the receiver by the transverse wind, much like the clouds moving overhead.

For a propagating infinite plane wave, the Taylor frozen turbulence hypothesis permits us to set $\rho = V\tau$ in the spatial covariance function, where τ is a time scale.

Temporal spectrum of irradiance fluctuations: Because the covariance is an *even* function, the **temporal spectrum** of irradiance fluctuations can be defined by the Fourier cosine transform

$$S_I(\omega) = 4\int_0^\infty B_I(V\tau)\cos\omega\tau d\tau$$
$$= \frac{4}{\omega_t}\int_0^\infty B_I(Vs/\omega_t)\cos\left(\frac{\omega s}{\omega_t}\right)ds,$$

where $\omega_t = V/\sqrt{L/k}$ represents the transition angular frequency at which the spectrum begins to decay under weak irradiance fluctuations.

To emphasize the distribution of power concentration of the irradiance fluctuations over various frequencies, the temporal spectrum is often first multiplied by frequency ω and then plotted.

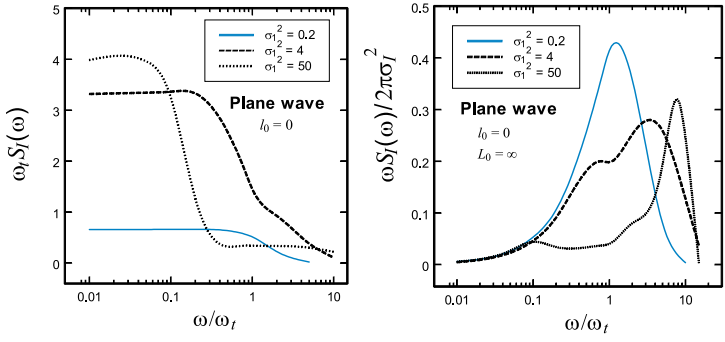

Aperture Averaging: Plane Wave

Aperture-averaging factor A: The ratio of the irradiance flux variance obtained by a finite-size receiver lens to that obtained by a point detector, i.e.,

$$A = \frac{\sigma_I^2(D)}{\sigma_I^2(0)} = \frac{16}{\pi}\int_0^1 b_I(Dx)\left(\cos^{-1}x - x\sqrt{1-x^2}\right)x\,dx,$$

where D is lens diameter and $b_I(\rho)$ is the **normalized covariance function** of irradiance fluctuations for a plane wave.

Weak fluctuations—under weak fluctuations the **aperture-averaging factor** can be approximated by

$$A = \left[1 + 1.06\left(\frac{kD^2}{4L}\right)\right]^{-7/6}, \quad \sigma_1^2 < 1.$$

Strong fluctuations—under both weak and strong irradiance fluctuation conditions, the **irradiance flux variance** can be approximated by

$$\sigma_I^2(D) \cong \exp\left[\frac{0.49\sigma_1^2}{(1+0.65d^2+1.11\sigma_1^{12/5})^{7/6}} + \frac{0.51\sigma_1^2(1+0.69\sigma_1^{12/5})^{-5/6}}{1+0.90d^2+0.62d^2\sigma_1^{12/5}}\right] - 1,$$

where $d = \sqrt{kD^2/4L}$.

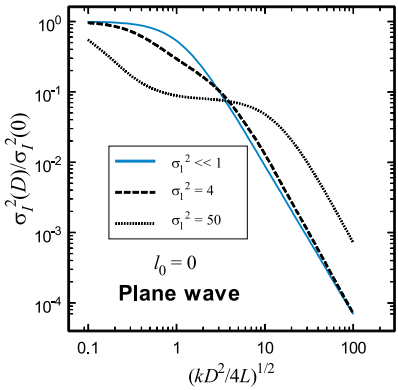

Aperture-averaging factor.

Aperture Averaging: Spherical Wave

Aperture-averaging factor A: The ratio of the irradiance flux variance obtained by a finite-size receiver lens to that obtained by a point detector, i.e.,

$$A = \frac{\sigma_I^2(D)}{\sigma_I^2(0)} = \frac{16}{\pi}\int_0^1 b_I(Dx)\left(\cos^{-1}x - x\sqrt{1-x^2}\right)x\,dx,$$

where D is lens diameter and $b_I(\rho)$ is the **normalized covariance function** of irradiance fluctuations for a spherical wave.

Strong fluctuations—under very general irradiance fluctuation conditions, the **irradiance flux variance** can be approximated by

$$\sigma_I^2(D) \cong \exp\left[\frac{0.49\beta_0^2}{(1+0.18d^2+0.56\beta_0^{12/5})^{7/6}} + \frac{0.51\beta_0^2(1+0.69\beta_0^{12/5})^{-5/6}}{1+0.90d^2+0.62d^2\beta_0^{12/5}}\right] - 1,$$

where $d = \sqrt{kD^2/4L}$.

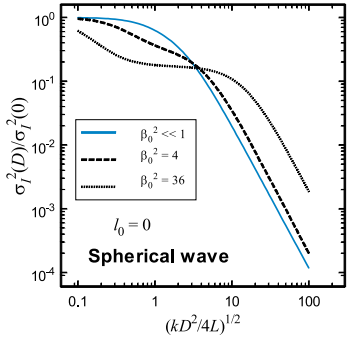

Aperture-averaging factor.

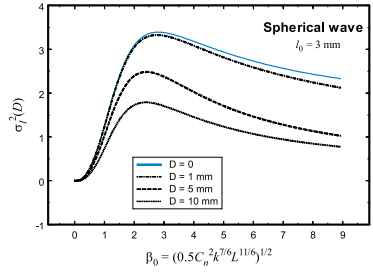

Irradiance flux variance vs. strength of turbulence and various aperture sizes. Here, λ = 0.633 μm, l_0 = 3 mm, and $C_n^2 = 5\times10^{-13}$ m$^{-2/3}$.

Example

A spherical wave is propagated through atmospheric turbulence to a receiver located 500 meters from the transmitter. Given that the wavelength is 0.5 μm and $C_n^2 = 0.5 \times 10^{-13}\ \text{m}^{-2/3}$,

(a) calculate the scintillation index at the receiver.
(b) If the receiver aperture is 4 cm in diameter, calculate the flux variance (reduced scintillation) in the plane of the detector.
(c) If the propagation distance is 1.5 km, what is the scintillation index and flux variance?

Solution: First calculate parameters:

$$L = 500 \text{ m}: \quad \beta_0^2 = 0.5 C_n^2 k^{7/6} L^{11/6} = 0.425,$$

$$d = \sqrt{\frac{kD^2}{4L}} = 3.17$$

$$L = 1500 \text{ m}: \quad \beta_0^2 = 3.186, \quad d = 1.83$$

(a) $$\sigma_I^2 = \exp\left[\frac{0.49\beta_0^2}{(1+0.56\beta_0^{12/5})^{7/6}} + \frac{0.51\beta_0^2}{(1+0.69\beta_0^{12/5})^{5/6}}\right] - 1$$

$$= 0.417$$

(b) $$\sigma_I^2(D) \cong \exp\left[\frac{0.49\beta_0^2}{(1+0.18d^2+0.56\beta_0^{12/5})^{7/6}} + \frac{0.51\beta_0^2(1+0.69\beta_0^{12/5})^{-5/6}}{1+0.90d^2+0.62d^2\beta_0^{12/5}}\right] - 1 = 0.075$$

(c) $\sigma_I^2 = 1.54, \quad \sigma_I^2(D) = 0.44$

Imaging Systems and Adaptive Optics

Electromagnetic wave absorption and scattering give rise to attenuation of the irradiance that affects the quality of images propagating through the atmosphere because of reduced contrast and image blurring of detail. Intensity and phase fluctuations due to atmospheric turbulence can also cause blurring and other effects that limit the practical utilization of optical instruments for astronomy, communications, lidar, telemetry, remote sensing, and other applications. The development of compensation methods for the turbulent distortions is of great importance in such applications.

Image degrading effects of an optical system can be described in terms of the **modulation transfer function** MTF and the **long-exposure resolution**, both of which depend on the **atmospheric coherence length** r_0. The atmospheric coherence length imposes a severe limit on the effective aperture size of the system.

Systems that use mechanical means to sense and correct for atmospherically induced wave front deformations in real time are called **adaptive optics systems**. The major components of an adaptive optics imaging (AOI) system are a deformable mirror, wave front sensor, and an actuator command computer. Among others, limiting factors that prevent AOI systems from achieving ideal performance are finite light levels in the wave front sensor and differences between the sensed wave front and that of the object being imaged (**anisoplanatism**).

Fried's Atmospheric Parameter and Greenwood's Time Constant

Fried parameter: In a vacuum, the far-field diffraction pattern has an angular extent (**seeing angle**) of λ/D, whereas in turbulence the seeing angle is λ/r_0, where r_0 is **Fried's atmospheric coherence length**

$$r_0 = \left[0.42 \sec(\zeta) k^2 \int_0^L C_n^2(z) dz\right]^{-3/5}.$$

Here, D is telescope diameter and ζ is the zenith angle.

- Fried's parameter r_0 is related to the plane wave **spatial coherence radius** by $r_0 = 2.1\rho_0$.
- At sea level, Fried's parameter r_0 is typically 2 to 15 cm at visible and IR wavelengths.
- An aperture of dimension r_0 produces a near-diffraction-limited image (which appears to change position as the atmosphere evolves in time).
- For vacuum propagation, the seeing angle λ/D for a 4-m telescope operating in the visible corresponds to 0.03 arc sec. Under good atmospheric seeing conditions, the "effective" seeing angle λ/r_0 may be only as small as 0.4 arc sec.

Temporal characteristics of turbulence are based on the frozen turbulence hypothesis.

Greenwood time constant—specifies the time interval over which turbulence remains essentially unchanged, i.e.,

$$\tau_0 = \frac{\cos^{3/5}(\zeta)}{[2.91 k^2 \int_{h_0}^{H} C_n^2(h) V^{5/3}(h) dh]^{3/5}},$$

where $V(h)$ is the wind-velocity profile as a function of altitude, h_0 is altitude of the receiver, and H is altitude of the source.

Point Spread Function and Modulation Transfer Function

Incoherent imaging system: A system that is linear with irradiance (rather than amplitude or field).

Point spread function PSF: The impulse response of an incoherent imaging system. For a circular aperture of diameter D and focal length f, the (normalized) point spread function in a vacuum is the **Airy disk** defined by

$$\mathrm{PSF}_0(r) = \left[\frac{J_1(Dr/2\lambda f)}{Dr/2\lambda f}\right]^2,$$

where $J_1(x)$ is a Bessel function.

Optical transfer function OTF: The normalized Fourier transform of the PSF, i.e., the transfer function of an incoherent imaging system.

Modulation transfer function MTF: The modulus of the OTF of an imaging system.

MTF of the imaging system in free space—(ν is spatial frequency):

$$\mathrm{MTF}_0(\nu) = \begin{cases} \dfrac{2}{\pi}[\cos^{-1}(\lambda f\nu/D) - (\lambda f\nu/D)\sqrt{1-(\lambda f\nu/D)^2}], \\ \quad \nu < D/\lambda f, \\ 0, \quad \nu > D/\lambda f. \end{cases}$$

Atmospheric MTF—in the atmosphere, the MTF is given by (neglecting aerosol scattering)

$$\mathrm{MTF}_{\mathrm{atm}}(\nu) = \exp\left[-3.44(\lambda f\nu/r_0)^{5/3}\right].$$

The overall MTF (free space and atmosphere) is defined by

$$\mathrm{MTF}_{\mathrm{total}}(\nu) = \mathrm{MTF}_0(\nu)\mathrm{MTF}_{\mathrm{atm}}(\nu).$$

Spatial Resolution

Spatial resolution: A measure of system performance that refers to the imaging system's ability to distinguish between two closely spaced point sources.

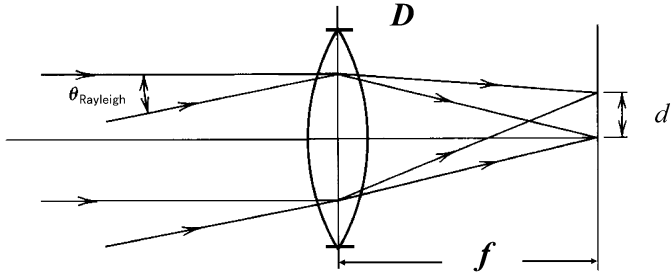

Blur circle—the actual image of a point source as defined by the diameter of the **Airy disk**, i.e.,

$$d = 2.44\frac{\lambda f}{D}.$$

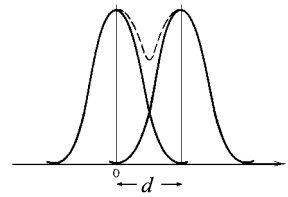

Intensity of two point images resolved by Rayleigh limit.

Rayleigh resolution—the distance to the first zero of the **Airy disk** is

$$r = 1.22\frac{\lambda f}{D},$$

and the **Rayleigh criterion** is given by the angular distance

$$\theta_{\text{Rayleigh}} = 1.22\frac{\lambda}{D}.$$

Sparrow resolution—another technique for defining optical resolution, viz.,

$$\theta_{\text{Sparrow}} = \frac{\lambda}{D}.$$

Strehl Ratio and Image Resolving Power

Strehl ratio: The ratio between the achieved on-axis beam irradiance and its diffraction limited value.

When the residual phase variance σ_ϕ^2 is small compared with unity, the Strehl ratio can be approximated by the **Maréchal approximation**

$$\mathrm{SR} = \exp(-\sigma_\phi^2) \approx 1 - \sigma_\phi^2.$$

Under more general conditions, the Strehl ratio leads to

$$\mathrm{SR} = \frac{1}{[1 + (D/r_0)^{5/3}]^{6/5}}.$$

Image jitter—arises from the overall tilt imparted to the optical wave front by the advection of large eddies.

Image blur—caused by both small-scale and large-scale effects.

Image blurring and image dancing (jitter) are associated primarily with large-scale phase fluctuations.

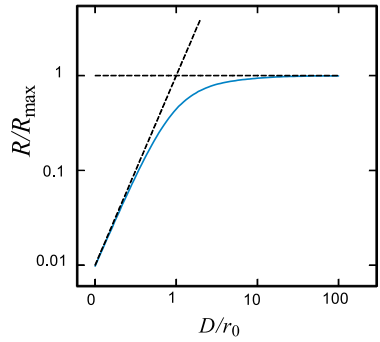

Long-exposure resolution—also known as **resolving power** R, it is another measure of imaging system performance defined by

$$\frac{R}{R_{\max}} \cong \frac{(D/r_0)^2}{[1 + (D/r_0)^{5/3}]^{6/5}},$$

where $R_{\max} = \pi r_0^2 / 4\lambda^2 f^2$.

Isoplanatic Angle and Point-Ahead Angle

The principle behind adaptive optics imaging AOI systems is to sense the phase distortions of a known source and apply a "corrective" or conjugate phase to the outgoing beam or incoming image.

Guide star—a beacon used to sense atmospheric phase distortion from the propagation path of an object being imaged.

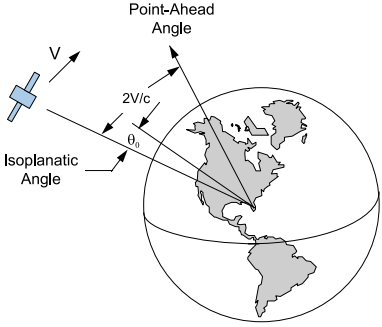

Isoplanatic angle: The angular distance (from the guide star) over which atmospheric turbulence is essentially unchanged is called the **isoplanatic angle** θ_0. If ζ is zenith angle and h is altitude, then the isoplanic angle is given by

$$\theta_0 = \frac{\cos^{8/5}(\zeta)}{[2.91k^2 \int_{h_0}^{H} C_n^2(h)(h-h_0)^{5/3}dh]^{3/5}}.$$

Angular anisoplanatism occurs when a moving uncooperative satellite target is being tracked by one beam and another is used to intercept the target at a **point-ahead angle**. This angle, which must allow for transit time from the satellite to the ground and back again, is $\theta_p = 2V/c$, where V is target speed and c is the speed of light.

The point-ahead angle is typically on the order of 50 μrad, which is ordinarily much larger than the isoplanatic angle from the tracking direction. For this reason, a measurement along the tracking path may not be useful in correcting for the turbulence along the propagation path. In this case a synthetic beacon or laser guide star may be necessary.

Zernike Polynomials and Wave Front Representation

Zernike polynomials represent an orthogonal set of functions of two variables over a unit circle

$$Z_n^m(r,\theta) = R_n^m(r)e^{im\theta},$$

where both m and n are integers, $n \geq 0$, $-n \leq m \leq n$, and $n \pm |m|$ is even, and

$$R_n^m(r) = \sum_{k=0}^{(n-|m|)/2} \frac{(-1)^k(n-k)!}{\left(\frac{n+m}{2}-k\right)!\left(\frac{n-m}{2}-k\right)!}\frac{r^{n-2k}}{k!}.$$

Lower-order Zernike polynomials are known as **piston**, **tilt**, **focus**, **astigmatism**, **coma**, and so forth. They are also useful in adaptive optics systems designed for atmospheric turbulence decomposition.

Virtually any realistic wave front $\Phi(r,\theta)$ can be represented in a **two-dimensional Fourier series** of Zernike polynomials

$$\Phi(r,\theta) = \sum_{n=0}^{\infty}\sum_{m=-n}^{n} C_{mn}R_n^m(r)e^{im\theta},$$

where C_{mn} are **Fourier coefficients**. The coefficient $C_{00} = \langle\Phi(r,\theta)\rangle$ is the **piston**, equal to the average value of the wave front.

Rms wave front error: The square root of the "mean-square" deformation of the wave front, given by

$$(\Delta\Phi)^2 = \sum_{n=1}^{\infty}\sum_{m=-n}^{n}\frac{|C_{mn}|^2}{n+1}.$$

Zernike Polynomials for Atmospheric Imaging

The form of the **Zernike polynomials** that is commonly used in studying atmospheric effects on imaging systems leads to

$$Z_i(r) \equiv Z_i[0,n] = \sqrt{n+1}R_n^0(r), \quad m = 0,$$
$$Z_{i,\text{even}}(r,\theta) \equiv Z_{i,\text{even}}[m,n] = \sqrt{n+1}R_n^m(r)\sqrt{2}\cos m\theta, \quad m \neq 0,$$
$$Z_{i,\text{odd}}(r,\theta) \equiv Z_{i,\text{odd}}[m,n] = \sqrt{n+1}R_n^m(r)\sqrt{2}\sin m\theta, \quad m \neq 0.$$

The ordering scheme for these polynomials uses the rule that, for a given n, the modes with smaller m are counted first:

- $Z_1[0,0]$ represents **piston**;
- $Z_2[1,1]$ and $Z_3[1,1]$ represent **wavefront tilt** in the x and y directions, respectively;
- $Z_4[0,2]$ is **focus** (or **defocus**);
- $Z_5[2,2]$ and $Z_6[2,2]$ are two components of **astigmatism**.

i	m	n	Zernike Polynomial $Z_i[m,n]$
1	0	0	1
2	1	1	$2r\cos\theta$
3	1	1	$2r\sin\theta$
4	0	2	$\sqrt{3}(2r^2-1)$
5	2	2	$\sqrt{6}r^2\sin 2\theta$
6	2	2	$\sqrt{6}r^2\cos 2\theta$
7	1	3	$\sqrt{8}(3r^3-2r)\sin\theta$
8	1	3	$\sqrt{8}(3r^3-2r)\cos\theta$
9	3	3	$\sqrt{8}r^3\sin 3\theta$
10	3	3	$\sqrt{8}r^3\cos 3\theta$

Modal Expansion and Aperture Filter Functions

Modal expansion: A series representation of the random wave front of the form

$$\Phi(2\rho/D, \theta) = \sum_{i=1}^{\infty} a_i Z_i(2\rho/D, \theta),$$

where D is the aperture diameter and a_i are the **Fourier coefficients**.

Mean-square phase error: If the first N Zernike modes in the wave front are removed, the resulting mean-square phase error is

$$\epsilon_N^2 = \sum_{i=N+1}^{\infty} \langle (a_i)^2 \rangle.$$

Filter functions are used to determine the effect of atmospheric turbulence for either a finite size source or receiver.

Complex filter functions: The two-dimensional Fourier transform of the Zernike polynomials scaled by the area of the aperture gives us

$$\left.\begin{matrix} G_i(\kappa) \\ G_{i,\text{even}}(\kappa, \phi) \\ G_{i,\text{odd}}(\kappa, \phi) \end{matrix}\right\} = \sqrt{n+1}\frac{2J_{n+1}(\kappa D/2)}{\kappa D/2} \left\{\begin{matrix} (-1)^{n/2} \\ (-1)^{(n-m)/2}\sqrt{2} i^m \cos m\phi \\ (-1)^{(n-m)/2}\sqrt{2} i^m \sin m\phi. \end{matrix}\right.$$

Aperture filter functions: The absolute value squared of the complex filter functions leads to

$$\left.\begin{matrix} F_i(\kappa) \\ F_{i,\text{even}}(\kappa, \phi) \\ F_{i,\text{odd}}(\kappa, \phi) \end{matrix}\right\} = (n+1)\left[\frac{2J_{n+1}(\kappa D/2)}{\kappa D/2}\right]^2 \left\{\begin{matrix} 1 (m = 0) \\ 2\cos^2 m\phi \\ 2\sin^2 m\phi. \end{matrix}\right.$$

Zernike Tilt, Piston, and Angle-of Arrival Jitter

Tilt jitter variance—the two-axis Zernike tilt given by

$$T_Z^2 = \frac{6.08}{D^{1/3}} \int_0^L C_n^2(z)dz = 0.36\left(\frac{D}{r_0}\right)^{5/3}\left(\frac{\lambda}{D}\right)^2.$$

Tilt phase variance—defined as the tilt variance divided by the factor $(4/kD)^2$, viz.,

$$\sigma_T^2 = 0.90\left(\frac{D}{r_0}\right)^{5/3}.$$

Phase variance with piston removed—the difference between total and piston variance, given by

$$\sigma_{PR}^2 = 1.03\left(\frac{D}{r_0}\right)^{5/3}.$$

Phase variance with piston and tilt removed—the difference between the total phase variance and that of the piston and tilt variance

$$\sigma_{PTR}^2 = 0.13\left(\frac{D}{r_0}\right)^{5/3}.$$

Angle-of-arrival jitter (dynamic tilt) of a beam wave on a target can occur even if a tracking system is doing a perfect job!

Angle-of-arrival tilt—residual tilt at the target given by

$$T_t^2 = \frac{6.08}{L^2D^{1/3}} \int_0^L C_n^2(z)z^2dz = 0.36\left(\frac{D}{r_0}\right)^{5/3}\left(\frac{\lambda}{D}\right)^2.$$

Free Space Optical Communication Systems

A **communication system** is designed to transmit and receive information. The information to be sent is generally superimposed by **modulation** onto an electromagnetic wave called a **carrier**. It is then transmitted to a receiver where the information is recovered by **demodulation**.

Compared with conventional RF systems, there are several significant advantages offered by **free space optical** FSO communication systems (also called **lasercom systems**) that are simple consequences of the short wavelengths (high frequencies) associated with optical waves. Among these advantages are the following:

- smaller antenna (telescope)
- smaller size and weight of the components
- power concentration in a very narrow beam (a more secure channel)
- potential increase in modulation bandwidth

Although the advantages listed above are based on shorter wavelengths, the disadvantages caused by atmospheric effects (haze, fog, snow, rain, and turbulence) are also a consequence of the shorter wavelengths.

Direct Detection System

A **direct detection system** is one that responds only to the instantaneous power of the collected field, also called an incoherent detection system or a power-detecting system.

The modulation format for the transmitted signal is generally intensity modulation.

Noise sources present throughout the receiver include

- background radiation (sun, blackbody, etc.)
- detector noise or shot noise
- circuit and electronic noise after photodetection.

The **photo-detector** converts the optical signal into an electrical signal for processing, and the **lowpass filter** eliminates much of the random noise.

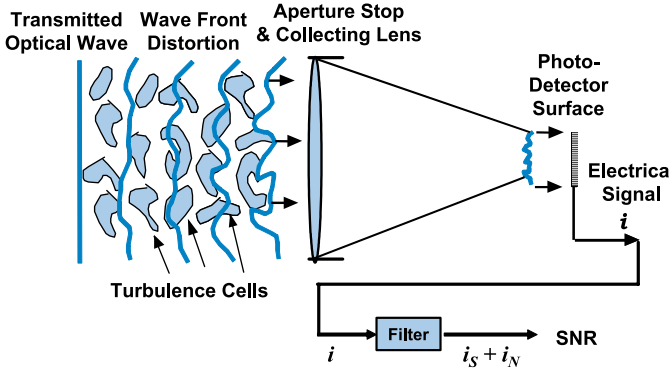

Direct detection system.

Threshold Detection

The need to determine the presence of a "signal" embedded in "noise" is fundamental in FSO communication systems.

- When the output of a detector exceeds a set threshold I_T, we say a **signal is present**.
- A **false alarm** arises when noise alone exceeds the threshold and is interpreted as "signal."
- When the signal plus noise does not exceed threshold, it is called **missed detection** (or probability of fade).

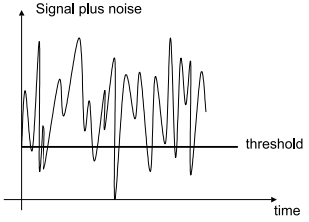

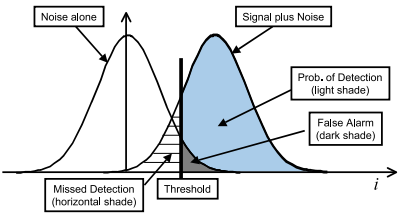

False alarm probability: For zero-mean Gaussian noise, this is defined by

$$\mathrm{Pr}_{\mathrm{fa}} = \int_{i_T}^{\infty} p_n(i)di = \frac{1}{2}\,\mathrm{erfc}\left(\frac{i_T}{\sqrt{2}\sigma_N}\right),$$

where i_T is the threshold and σ_N is rms noise power.

Detection probability: defined by

$$\mathrm{Pr}_{\mathrm{d}} = \int_{i_T}^{\infty} p_{s+n}(i)di = \frac{1}{2}\,\mathrm{erfc}\left(\frac{i_T - i_S}{\sqrt{2}\sigma_N}\right).$$

Signal-to-Noise Ratio: Direct Detection

The performance of a receiver is often based on the notion of **signal-to-noise ratio** SNR, i.e., the rms signal power over the rms noise power.

For photon-noise limited performance, the **mean SNR** for a direct detection system is

$$\langle \mathrm{SNR} \rangle = \frac{\mathrm{SNR}_0}{\sqrt{\frac{P_{S0}}{\langle P_S \rangle} + \sigma_I^2(D)\mathrm{SNR}_0^2}},$$

where P_{S0} is the signal power in free space, $\langle P_S \rangle$ is the mean signal power, $\sigma_I^2(D)$ is the irradiance flux variance for an aperture of diameter D, and SNR_0 is the **free-space SNR** defined by

$$\mathrm{SNR}_0 = \sqrt{\frac{\eta P_{S0}}{2h\nu B}} \quad \text{(free space)}.$$

η = detector quantum efficiency (electrons/photon)
e = electric charge (Coulombs/electron)
$h = 6.63 \times 10^{-34}$ joule-sec (Planck's constant)
ν = optical frequency (Hertz)
B = bandwidth (Hertz)

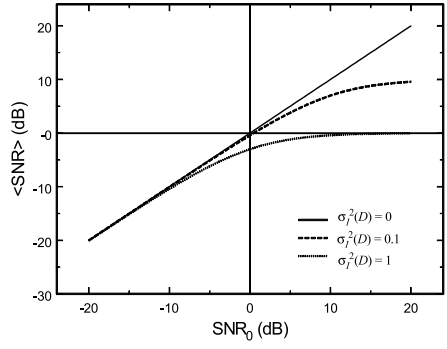

Bit Error Rate

System performance for continuous wave CW or single-pulse optical systems is based on **SNR** and **fade probability**.

For **digital transmission** of information, the performance measure is based on the **probability of error**, also called the **bit error rate** BER.

On-off keying binary detection system OOK: The most basic form of pulsed modulation. In the presence of optical turbulence, the BER is

$$\Pr(E) = \frac{1}{2}\int_0^\infty p_I(x)\,\mathrm{erfc}\left(\frac{\langle \mathrm{SNR}\rangle x}{2\sqrt{2}\langle i_S\rangle}\right)dx,$$

where $\langle i_S\rangle$ is the mean signal current out of the detector, $\langle \mathrm{SNR}\rangle$ is the mean SNR, and $p_I(x)$ is the PDF for atmospheric irradiance fluctuations.

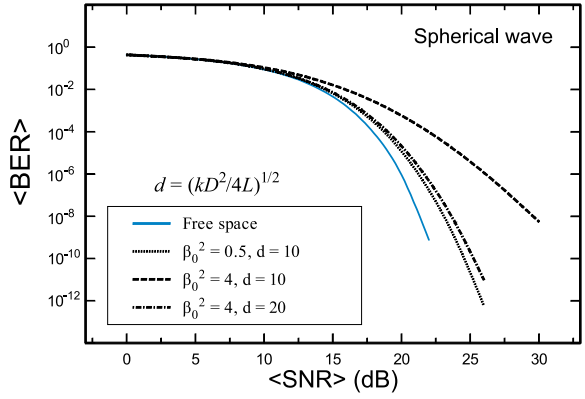

Coherent Detection System

A **coherent detection system** uses a local oscillator LO at the receiver to downconvert the carrier to baseband (homodyne) or to an intermediate IF carrier (heterodyne).

The modulation format can include (i) amplitude modulation, (ii) frequency modulation, and (iii) phase modulation.

Primary **noise source** is LO.

The **mean carrier-to-noise ratio** CNR for a heterodyne receiver of aperture diameter D at the output of the IF filter is

$$\langle \text{CNR} \rangle \cong \frac{\text{CNR}_0}{[1 + (D/r_0)^{5/3}]^{6/5}},$$

where r_0 is Fried's parameter and CNR_0 is the CNR in free space given by

$$\text{CNR}_0 = \frac{\epsilon \eta P_{S0}}{h\nu B}.$$

$\epsilon =$ heterodyne efficiency (dimensionless)
$\eta =$ detector quantum efficiency (electrons/photon)

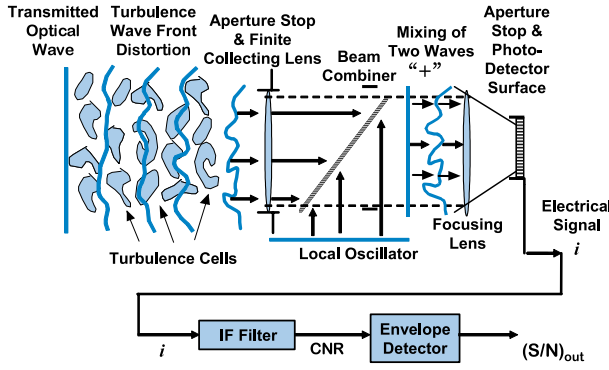

Signal-to-Noise Ratio: Coherent Detection

In a **heterodyne coherent detection system**, the performance of a system can be evaluated either on the basis of CNR at the IF filter output or evaluated by the SNR at the low-pass filter output of the envelope detector.

A heterodyne receiver has a second level of detection at baseband in the form of an **envelope detector** (linear or square-law).

The concept of SNR at the output of the envelope detector is somewhat ambiguous because of the mixing of signal and noise terms, leading to components of the type $n \times n$ (those due to the noise beating with itself) and of the type $s \times n$ (those due to the noise beating with the signal).

The **mean SNR** at the lowpass output of a square-law detector is

$$\left(\frac{S}{N}\right)_{\text{out}} = \frac{\langle \text{CNR} \rangle^2}{1 + 2\langle \text{CNR} \rangle + \sigma_I^2(D)\langle \text{CNR} \rangle^2},$$

where $\sigma_I^2(D)$ is the flux variance at the detector.

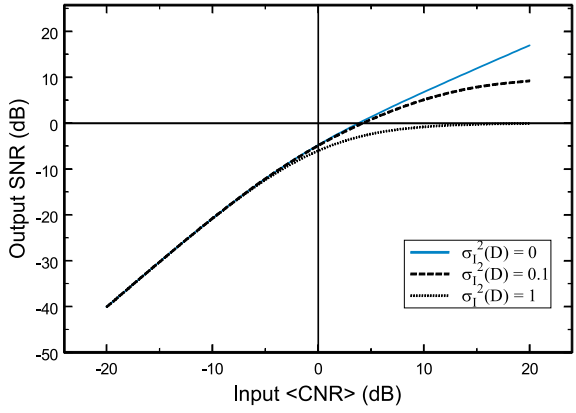

Probability of Fade: Lognormal Model

The fade statistics given below are for a single point in the pupil plane of a receiving system.

Lognormal model—conventional model for weak irradiance fluctuations given by

$$p_I(I) = \frac{1}{I\sigma_I(r,L)\sqrt{2\pi}} \times \exp\left\{ -\frac{\left[\ln\left(\frac{I}{\langle I(r,L)\rangle}\right) + \frac{1}{2}\sigma_I^2(r,L)\right]^2}{2\sigma_I^2(r,L)} \right\}, \quad I > 0.$$

Probability of fade (or fractional fade time): Describes the percentage of time that the irradiance of the received wave is below a prescribed threshold. For a lognormal model,

$$\Pr(I \le I_T) = \frac{1}{2}\left\{ 1 + \operatorname{erf}\left[\frac{\frac{1}{2}\sigma_I^2(r,L) + \frac{2r^2}{W_e^2} - 0.23F_T}{\sqrt{2}\sigma_I(r,L)} \right] \right\}.$$

I_T = threshold
F_T = fade irradiance level I_T below the mean in dB
W_e = effective spot radius in turbulence

Expected number of fades (surges) per second: For a lognormal model is

$$\langle n(I_T)\rangle = \nu_0 \exp\left\{ -\frac{\left[\frac{1}{2}\sigma_I^2(r,L) + \frac{2r^2}{W_e^2} - 0.23F_T\right]^2}{2\sigma_I^2(r,L)} \right\},$$

where ν_0 is a quasi-frequency often taken as 550 Hz.

Mean fade time: $\langle t(I_T)\rangle = \dfrac{\Pr(I \le I_T)}{\langle n(I_T)\rangle}$.

Probability of Fade: Gamma-Gamma Model

Gamma-gamma model—general model for weak or strong irradiance fluctuations given by

$$p_I(I) = \frac{2(\alpha\beta)^{(\alpha+\beta)/2}}{\Gamma(\alpha)\Gamma(\beta)I}\left(\frac{I}{\langle I(\mathbf{r},L)\rangle}\right)^{(\alpha+\beta)/2} \times K_{\alpha-\beta}\left(2\sqrt{\frac{\alpha\beta I}{\langle I(\mathbf{r},L)\rangle}}\right), \quad I>0.$$

The parameters α and β for a spherical wave incident on a receiver of aperture diameter D are

$$\alpha = \frac{1}{\exp\left[\dfrac{0.49\beta_0^2}{(1+0.18d^2+0.56\beta_0^{12/5})^{7/6}}\right]-1},$$

$$\beta = \frac{1}{\exp\left[\dfrac{0.51\beta_0^2(1+0.69\beta_0^{125})^{-5/6}}{1+0.90d^2+0.62d^2\beta_0^{12/5}}\right]-1},$$

where $\beta_0^2 = 0.5C_n^2k^{7/6}L^{11/6}$ and $d=\sqrt{kD^2/4L}$.

Probability of fade (or fractional fade time): Describes the percentage of time that the irradiance of the received wave is below a prescribed threshold. For a gamma-gamma model, it is recommended to use numerical integration to calculate

$$\Pr(I \le I_T) = \int_0^{I_T} p_I(I)dI.$$

Expected number of fades (surges) per second for a gamma-gamma model is

$$\langle n(I_T)\rangle = \frac{2\sqrt{2\pi\alpha\beta}\nu_0\sigma_I}{\Gamma(\alpha)\Gamma(\beta)}\left(\frac{\alpha\beta I_T}{\langle I\rangle}\right)^{(\alpha+\beta-1)/2} K_{\alpha-\beta}\left(2\sqrt{\frac{\alpha\beta I_T}{\langle I\rangle}}\right),$$

where ν_0 is a quasi-frequency often taken as 550 Hz.

Mean fade time: $\langle t(I_T)\rangle = \dfrac{\Pr(I \le I_T)}{\langle n(I_T)\rangle}$.

Lasersatcom: Mean Irradiance and Beam Spreading

Mean irradiance: The ensemble average of the Gaussian-beam wave at the receiver plane, approximated by

$$\langle I(r, L)\rangle = \frac{W_0^2}{W_e^2}\exp(-2r^2/W_e^2),$$

where W_e is the long-time-average beam radius.

Uplink beam radius—for an uplink path of length L

$$W_e = W\sqrt{1 + 4.35\Lambda^{5/6}k^{7/6}(H - h_0)^{5/6}\sec^{11/6}(\zeta)\mu_1},$$

where ζ is zenith angle, $\Lambda = 2L/kW^2$, W is the free-space spot radius, and

$$\mu_1 = \int_{h_0}^{H} C_n^2(h)\left(1 - \frac{h - h_0}{H - h_0}\right)^{5/3} dh.$$

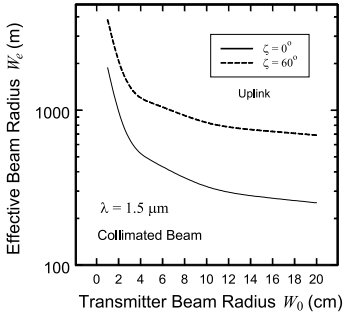

For H-$V_{5/7}$ C_n^2 model, $\mu_1 \cong 1.75 \times 10^{-11}$ m. ($H > 20$ km)

Downlink beam radius—for a downlink path

$$W_e \cong W.$$

For a downlink path there is essentially no beam spreading beyond diffraction effects because the atmosphere is only close to the receiver.

Lasersatcom: Uplink Scintillation under Weak Fluctuations

Uplink scintillation—for zenith angles $\zeta \leq 45°$, the uplink scintillation index based on Rytov theory is defined by

$$\sigma_I^2(r,L) = 8.702k^{7/6}(H-h_0)^{5/6}\sec^{11/6}(\zeta) \times \left[\mu_{lu} + 1.667\frac{\mu_{ru}\Lambda^{5/6}\alpha^2(H-h_0)^2\sec^2(\zeta)}{W_0^2(\Theta_0^2+\Lambda_0^2)}\right], \quad \alpha \leq W/L,$$

where $\alpha = r/L$ is the radial angle distance from beam center,

$$\mu_{lu} = \mathrm{Re}\int_{h_0}^{H} C_n^2(h)\left\{\xi^{5/6}[\Lambda\xi + i(1-\overline{\Theta}\xi)]^{5/6} - \Lambda^{5/6}\xi^{5/3}\right\}dh,$$

$$\mu_{ru} = \int_{h_0}^{H} C_n^2(h)\left(1-\frac{h-h_0}{H-h_0}\right)^{5/3}dh,$$

and $\xi = 1-(h-h_0)/(H-h_0)$.

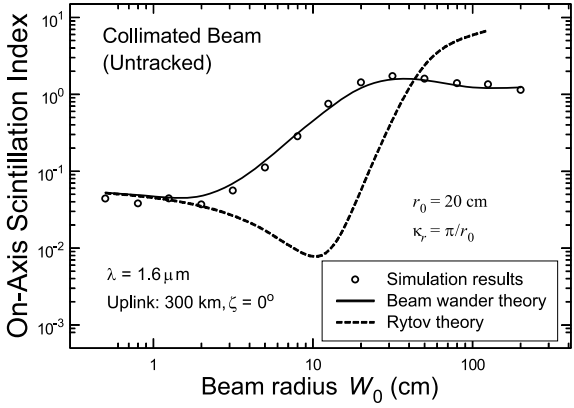

Uplink scintillation index for Rytov theory and with beam wander effects. (Simulation data courtesy of G. Baker.)

Lasersatcom: Downlink Scintillation under Weak Fluctuations

Downlink scintillation—for zenith angles $\zeta \le 45°$, the downlink scintillation index is defined by

$$\sigma_I^2(r,L) = 8.702k^{7/6}(H-h_0)^{5/6}\sec^{11/6}(\zeta) \times \left[\mu_{ld} + 1.667\frac{\mu_{rd}\Lambda^{5/6}\alpha^2(H-h_0)^2\sec^2(\zeta)}{W_0^2(\Theta_0^2+\Lambda_0^2)}\right], \quad \alpha \le W/L,$$

where $\alpha = r/L$ is the radial angle distance from beam center,

$$\mu_{ld} = \mathrm{Re}\int_{h_0}^{H} C_n^2(h)\left\{\xi^{5/6}\left[\Lambda\xi + i(1-\overline{\Theta}\xi)\right]^{5/6} - \Lambda^{5/6}\xi^{5/3}\right\}dh,$$

$$\mu_{rd} = \int_{h_0}^{H} C_n^2(h)\left(\frac{h-h_0}{H-h_0}\right)^{5/3}dh,$$

and $\xi = (h-h_0)/(H-h_0)$.

For transmitters in which $H \gg 20$ km the downlink scintillation index is essentially that of an unbounded plane wave (no radial dependence).

For zenith angles $0° \le \zeta \le 60°$, the scintillation index across the beam profile for downlink channels is typically

$$\sigma_I^2(r,L) \sim 0.07 \text{ to } 0.23, \quad 0 \le r < W$$

out to the diffraction-limited beam edge, regardless of initial beam size.

Lasersatcom: General Theory for Uplink/Downlink Scintillation

For a **downlink plane wave**, the scintillation index for *any* zenith angle is given by

$$\sigma_I^2 = \exp\left[\frac{0.49\sigma_1^2}{(1+1.11\sigma_1^{12/5})^{7/6}} + \frac{0.51\sigma_1^2}{(1+0.69\sigma_1^{12/5})^{5/6}}\right] - 1,$$

where

$$\sigma_1^2 = 2.25\mu_{\rm pl}k^{7/6}(H-h_0)^{5/6}\sec^{11/6}(\zeta),$$

$$\mu_{\rm pl} = \int_{h_0}^{H} C_n^2(h)\left(\frac{h-h_0}{H-h_0}\right)^{5/6} dh.$$

For H-$V_{5/7}$ C_n^2 model,
$\mu_{\rm pl} \cong 2.60 \times 10^{-16}$ m$^{1/3}$.
($H > 20$ km)

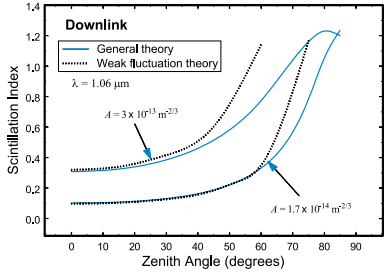

For an **uplink spherical wave**, the scintillation index for any zenith angle is given by

$$\sigma_I^2 = \exp\left[\frac{0.49\sigma_2^2}{(1+0.56\sigma_2^{12/5})^{7/6}} + \frac{0.51\sigma_2^2}{(1+0.69\sigma_2^{12/5})^{5/6}}\right] - 1,$$

where $\sigma_2^2 = 2.25\mu_{\rm sp}k^{7/6}(H-h_0)^{5/6}\sec^{11/6}(\zeta)$,

$$\mu_{\rm sp} = \int_{h_0}^{H} C_n^2(h)\left(\frac{h-h_0}{H-h_0}\right)^{5/6} \times \left(1-\frac{h-h_0}{H-h_0}\right)^{5/6} dh,$$

$\mu_{\rm sp} \cong \mu_{\rm pl}$, ($H > 20$ km)

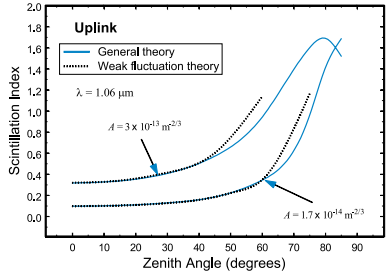

Lasersatcom: General Theory for Downlink Covariance and Correlation Width

The correlation width ρ_c for an uplink path to a satellite is many times larger than the probable size of any satellite.

For a **downlink plane wave**, the intensity covariance for any zenith angle is given by

$$B_I(\rho) = \exp\left[\sigma_{\ln x}^2 \frac{\mu_2(\rho)}{\mu_2(0)} + 0.99\sigma_{\ln y}^2 \left(\frac{k\rho^2\eta_y}{L}\right)^{5/12} \times K_{5/6}\left(\sqrt{\frac{k\rho^2\eta_y}{L}}\right)\right],$$

where

$$\sigma_{\ln x}^2 = \frac{0.49\sigma_1^2}{(1+1.11\sigma_1^{12/5})^{7/6}}, \qquad \sigma_{\ln y}^2 = \frac{0.51\sigma_1^2}{(1+0.69\sigma_1^{12/5})^{5/6}},$$

$$\mu_2(\rho) = \int_{h_0}^{H} \frac{C_n^2(h)\xi^{-1/3}}{\left(1-\frac{5}{8}\xi\right)^{7/5}} {}_1F_1\left[\frac{7}{5}; 1; \frac{-k\rho^2\eta_x}{8L\xi^{5/3}\left(1-\frac{5}{8}\xi\right)}\right] dh,$$

$$\eta_x = 0.92/(1+1.11\sigma_1^{12/5}), \qquad \eta_y = 3(1+0.69\sigma_1^{12/5}).$$

The **correlation width** ρ_c for a downlink path from a satellite is the $1/e^2$ point of the normalized covariance, $b_I(\rho_c) = B_I(\rho_c)/B_I(0) = 1/e^2$. It can be approximated under weak irradiance fluctuations by the empirical formula

$$\rho_c \cong \sqrt{\frac{45\times 10^3 \sec(\zeta)}{k}}, \quad \sigma_1^2 \ll 1. \quad [\text{m}]$$

Laser Radar and Optical Remote Sensing

Laser radar or **lidar systems** are a direct extension of conventional microwave radars to wavelengths from the optical bands. Such systems are capable of simultaneous measurements of range, reflectivity, velocity, temperature, azimuth, and elevation angle. A **monostatic system** is one in which the transmitter and receiver are co-located; in this setting the transmitter/receiver combination is often referred to as a transceiver. When the transmitter and receiver are separated in space by much more than a Fresnel zone, it is called a **bistatic system**.

An important application of atmospheric optics is **optical remote sensing**, which concerns the use of a laser beam to remotely sense information about the atmosphere. In particular, a coherent Doppler lidar can be used to measure the Doppler shift of backscattered lidar returns from the atmosphere. Such a system is able to remotely measure atmospheric wind speed with spatial resolution on the order of 100 m, or perhaps detect wind shear such as that in front of an aircraft.

Basic Radar Principles

Radar is concerned with the extraction of target information contained in the received signal—location, velocity, and target classification.

Pulse repetition frequency PRF—the PRF f_R is the number of pulses of temporal width τ transmitted per second.

Pulse repetition interval PRI—reciprocal of PRF which defines the period T.

Duty cycle—fraction of time that the radar is transmitting, i.e., τ/T.

Range equation: The basic equation of conventional radar

$$P_S = \frac{K}{L^4},$$

where P_S is received signal power, L is target range, and K is a constant.

Because laser radars generally operate in the near field, the range equation is usually modified to power law relations like $1/L^2$ or $1/L^3$. For example, for a Lambertian target of diameter D, the range equation becomes $P_S = \pi P_0 T_0^2 D^2/(4L)^2$, where P_0 is transmitted power and T_0 is the target reflection coefficient.

Maximum unambiguous range—$L_{\max} = \dfrac{c}{2f_R}$.

Doppler frequency shift—$f_d = -2V_r/\lambda$, where V_r is the relative (radial) speed of the target.

Maximum unambiguous velocity—$V_{r,\max} = \dfrac{\lambda f_R}{2}$.

Statistical Characteristics of Echo Beam

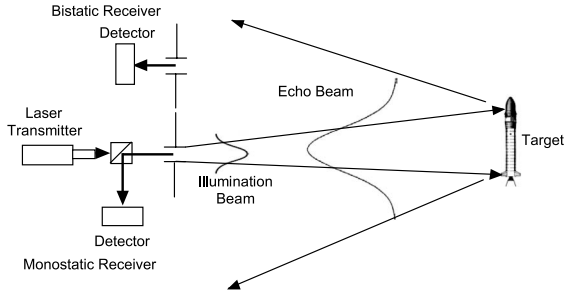

Laser radar configuration.

Target classifications—typical targets include aircraft, spacecraft, satellites, ships, ground vehicles, buildings, etc.

i. A **specular target** is usually considered to be smooth.
ii. A **diffuse target** is one with surface roughness correlation width comparable with the wavelength.
iii. An **unresolved target** lies entirely within the illumination beam.
iv. A **resolved** or **extended target** is larger than the illumination beam.

Target return beam spread—the reflected wave may experience considerable beam spreading along the path back to the receiver, particularly for smaller targets. The most significant effect will be loss of power.

Receiver plane loss of spatial coherence—for a small unresolved target the transverse spatial coherence radius of the return wave will be determined by the spatial coherence of an echo spherical wave. For a diffuse target the spatial coherence radius of the return optical wave may be greatly diminished over that of the illumination wave on the target, depending on the size of the target: larger targets lead to a greater loss of spatial coherence.

Receiver plane scintillation—will result in loss of signal-to-noise ratio and dropouts (information loss).

Enhanced Backscatter: Spherical Wave

Enhanced backscatter EBS: The increase in mean irradiance close to the optical axis in a monostatic laser radar system, caused by correlations between the incident and echo waves propagating through the same atmospheric turbulence in opposite directions.

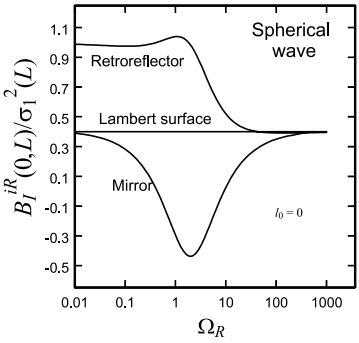

Scaled EBS correlation function under weak fluctuations for various reflectors.

Incident spherical wave (weak irradiance fluctuations)—for a smooth target of radius W_R, the return echo has the following characteristics:

Spot size: $$W_e = W_R\sqrt{(4+\Omega_R^2)\left[1+2.65\sigma_1^2\left(\frac{\Omega_R}{4+\Omega_R^2}\right)^{5/6}\right]}$$

EBS:

$$\frac{\langle I(0,2L)\rangle}{I(0,2L)_{\text{uncorr}}} = \exp\left[B_I^{iR}(0,L)\right]$$

$$= \exp\left[0.4\sigma_1^2 - 2.65\left(\frac{\Omega_R}{4+\Omega_R^2}\right)^{5/6}\sigma_1^2\right],$$

where $\Omega_R = 2L/kW_R^2$.

Incident spherical wave (general irradiance fluctuations)—for an unresolved target:

EBS: $$\frac{\langle I(0,2L)\rangle}{I(0,2L)_{\text{uncorr}}} = \exp\left[\frac{0.49\beta_0^2}{(1+0.56\beta_0^{12/5})^{7/6}} + \frac{0.51\beta_0^2}{(1+0.69\beta_0^{12/5})^{5/6}}\right]$$

$$= \begin{cases} 1+\beta_0^2, & \beta_0^2 \ll 1 \\ 2+\dfrac{1.89}{\beta_0^{4/5}}, & \beta_0^2 \gg 1 \end{cases}$$

Enhanced Backscatter: Gaussian-Beam Wave

Incident Gaussian-beam wave (weak irradiance fluctuations) for an **unresolved target** ($\Omega_R \gg 1$), the enhanced backscatter (EBS) is described approximately by

$$\frac{\langle I(0,2L)\rangle}{I(0,2L)_{\text{uncorr}}} = \exp\left[B_I^{iR}(0,L)\right] \cong 1 + \sigma_{B,C}^2,$$

where

$$\sigma_{B,C}^2 = 1.54\sigma_1^2\left[(1+\Theta_1)^2 + \Lambda_1^2\right]^{5/12} \cos\left[\frac{5}{6}\tan^{-1}\left(\frac{1+\Theta_1}{\Lambda_1}\right)\right]$$

$$- 1.49\sigma_1^2(\Theta_1^2 + \Lambda_1^2)^{5/12} \cos\left[\frac{5}{6}\tan^{-1}\left(\frac{\Theta_1}{\Lambda_1}\right)\right].$$

Incident Gaussian-beam wave (general irradiance fluctuations) for an **unresolved target** ($\Omega_R \gg 1$), the enhanced back-scatter EBS is

$$\frac{\langle I(0,2L)\rangle}{I(0,2L)_{\text{uncorr}}} = \exp\left[\frac{\sigma_{B,C}^2}{(1+0.58\sigma_{B,C}^{12/5})^{7/6}}\right]$$

$$\cong 2 + \frac{1.89}{\sigma_{B,C}^{4/5}}, \quad \sigma_{B,C}^2 \gg 1.$$

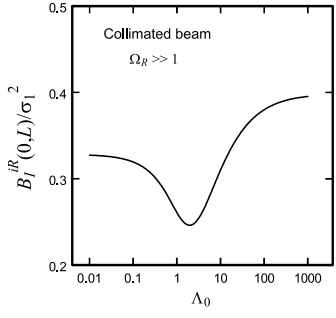

Scaled correlation function under weak fluctuations.

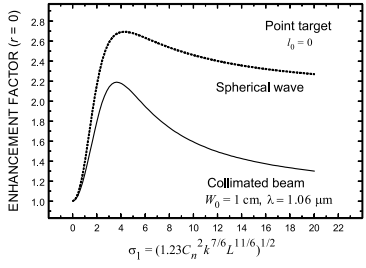

Enhancement factor as a function of strength of turbulence σ_1.

Spatial Coherence

For finite smooth targets, the **spatial coherence radius** of a monostatic echo return may be either greater than or less than that of the same wave in a bistatic channel, depending on target characteristics.

Point target—the wave structure function WSF for the echo wave from a small unresolved target is the same as that of a spherical wave propagating one way; hence, the **spatial coherence radius** is

$$\rho_0 \equiv \rho_{\text{sph}} = \frac{1}{(0.55C_n^2k^2L)^{3/5}}, \quad l_0 \ll \rho_0 \ll L_0, \quad C_n^2 = \text{const.}$$

Incident spherical wave (weak irradiance fluctuations)—the implied **spatial coherence radius** of a backscattered spherical wave in a monostatic channel is illustrated in the figure for a smooth target (mirror), retroreflector, and for a bistatic channel (either target):

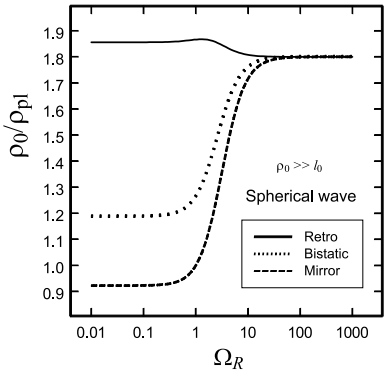

Spatial coherence radius scaled by the plane wave coherence radius for a reflected spherical wave.

Incident spherical wave (strong irradiance fluctuations)—the implied **spatial coherence radius** of a backscattered spherical wave in a monostatic channel is ($C_n^2 =$ const.)

$$\rho_0 = \begin{cases} 1.6(1.46C_n^2k^2L)^{-3/5}, & \Omega_R \ll 1 \\ 2.46(1.46C_n^2k^2L)^{-3/5}, & \Omega_R \gg 1 \end{cases}$$

Scintillation Index: Spherical Wave and Point Target

If a spherical wave illuminates a small unresolved target, the **scintillation index** associated with the echo wave is

$$\sigma_I^2(r, 2L) = \begin{cases} \sigma_{I,\mathrm{sph}}^2(L)\left[2 + \sigma_{I,\mathrm{sph}}^2(L)\right], \\ \quad \text{bistatic channel: } r \gg \sqrt{L/k} \\ \sigma_{I,\mathrm{sph}}^2(L)\left[4 + \sigma_{I,\mathrm{sph}}^2(L)\right], \\ \quad \text{monostatic channel: } r = 0 \end{cases}$$

where $l_0 = 0$, $L_0 = \infty$

$$\sigma_{I,\mathrm{sph}}^2(L) = \exp\left[\frac{0.49\beta_0^2}{(1 + 0.56\beta_0^{12/5})^{7/6}} + \frac{0.51\beta_0^2}{(1 + 0.69\beta_0^{12/5})^{5/6}}\right] - 1,$$

$$0 \le \beta_0^2 < \infty.$$

Strong irradiance fluctuations—in the saturation regime, the scintillation index approaches the asymptotic results

$$\sigma_I^2(r, 2L) \cong \begin{cases} 3 + \dfrac{7.6}{\beta_0^{4/5}}, \quad \beta_0^2 \gg 1 \\ \quad \text{bistatic channel: } r \gg \sqrt{L/k} \\ 5 + \dfrac{11.4}{\beta_0^{4/5}}, \quad \beta_0^2 \gg 1 \\ \quad \text{monostatic channel: } r = 0 \end{cases}$$

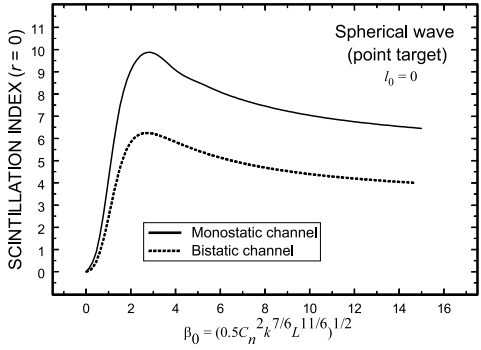

The echo wave scintillati on index of a spherical wave reflected from a small unresolved target.

Scintillation Index: Gaussian-Beam Wave and Point Target

The **scintillation index** associated with the echo wave of a collimated beam reflected from a small unresolved target is composed of three terms (weak irradiance fluctuations):

$$\sigma_I^2(r,2L)=\sigma_{I,\text{beam}}^2(0,L)+\sigma_{I,\text{sph}}^2(L)+2C_I^{iR}(r,L),\quad \Omega_R\gg 1$$

where $\sigma_{I,\text{sph}}^2(L)=0.4\sigma_1^2$, and

$$\sigma_{I,\text{beam}}^2(0,L)=3.86\sigma_1^2\left\{0.4\left[(1+2\Theta_1)^2+4\Lambda_1^2\right]^{5/12}\times\cos\left[\frac{5}{6}\tan^{-1}\left(\frac{1+2\Theta_1}{2\Lambda_1}\right)\right]-\frac{11}{16}\Lambda_1^{5/6}\right\},$$

$$C_I^{iR}(0,L)=1.54\sigma_1^2\left[(1+\Theta_1)^2+\Lambda_1^2\right]^{5/12}\times\cos\left[\frac{5}{6}\tan^{-1}\left(\frac{1+\Theta_1}{\Lambda_1}\right)\right]-1.49\sigma_1^2(\Theta_1^2+\Lambda_1^2)^{5/12}\cos\left[\frac{5}{6}\tan^{-1}\left(\frac{\Theta_1}{\Lambda_1}\right)\right].$$

Plane wave limit—in the limit $\Theta_1=1$, $\Lambda_1=0$, the on-axis scintillation of the echo wave reduces to

$$\sigma_I^2(r,2L)=\begin{cases}1.4\sigma_1^2, & \text{bistatic channel: } r\gg\sqrt{L/k}\\ 2.06\sigma_1^2, & \text{monostatic channel: } r=0\end{cases}$$

Spherical wave limit—in the limit $\Theta_1=0$, $\Lambda_1=0$, the on-axis scintillation of the echo wave reduces to

$$\sigma_I^2(r,2L)=\begin{cases}0.8\sigma_1^2, & \text{bistatic channel: } r\gg\sqrt{L/k}\\ 1.6\sigma_1^2, & \text{monostatic channel: } r=0\end{cases}$$

Scintillation Index: Smooth Target

Incident Gaussian-beam wave (weak fluctuations)—on the optical axis of an echo Gaussian-beam wave:

$$\sigma_L^2(0,2L) = 15.44\sigma_1^2\left\{0.4\left[(1+2\Theta_2)^2+4\Lambda_2^2\right]^{5/12} \times \cos\left[\frac{5}{6}\tan^{-1}\left(\frac{1+2\Theta_2}{2\Lambda_2}\right)\right] - \frac{11}{16}\Lambda_2^{5/6}\right\} + \sigma_{I,i}^2(0,L) + 2C_I^{iR}(0,L),$$

where $\sigma_{I,i}^2(0,L)$ and $2C_I^{iR}(0,L)$ are additional terms and

$$\Theta_2 = \frac{2-\Theta_1}{(2-\Theta_1)^2+(\Lambda_1+\Omega_R)^2},$$

$$\Lambda_2 = \frac{\Lambda_1+\Omega_R}{(2-\Theta_1)^2+(\Lambda_1+\Omega_R)^2}.$$

Plane wave limit—in the limit $\Theta_1 = 1$, $\Lambda_1 = 0$, the beam parameters above reduce to the plane wave limit

$$\Theta_2 = \frac{1}{1+\Omega_R^2}, \quad \Lambda_2 = \frac{\Omega_R}{1+\Omega_R^2}.$$

Spherical wave limit—in the limit $\Theta_1 = 0$, $\Lambda_1 = 0$, the scintillation index becomes

$$\sigma_I^2(0,2L) = 15.44\sigma_1^2\,\mathrm{Re}\left[i^{5/6}\,{}_2F_1\left(-\frac{5}{6},\frac{11}{6};\frac{17}{6};\overline{\Theta}_2+i\Lambda_2\right) - \frac{11}{16}\Lambda_2\right].$$

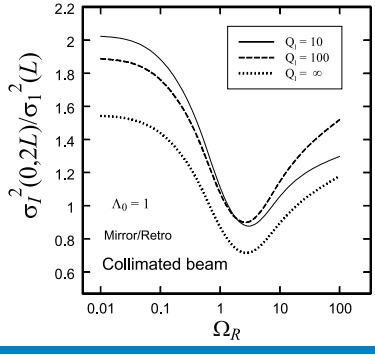

Scaled scintillation index on the optical axis vs. Ω_R and inner-scale parameter $Q_l = 10.89L/kl_0^2$.

Scintillation Index: Diffuse Target—I

Here we assume the characteristic correlation time τ_c associated with fluctuations in surface irregularities in the target is much shorter than the time constant τ_d of the detector (i.e., $\tau_c \ll \tau_d$).

Incident spherical wave—if a spherical wave illuminates a diffuse (Lambertian) target of radius W_R, the **scintillation index** associated with the echo wave in a **bistatic channel** is

$$\sigma_I^2(r, 2L)_{\text{bistatic}} = \sigma_{\text{diff}}^2(L)[2 + \sigma_{\text{diff}}^2(L)], \quad r \gg \sqrt{L/k},$$

where $d_R = \sqrt{kW_R^2/L}$,

$$\sigma_{\text{diff}}^2(L) = \exp\left[\frac{0.49\beta_0^2}{(1 + 0.18d_R^2 + 0.56\beta_0^{12/5})^{7/6}} + \frac{0.51\beta_0^2(1 + 0.69\beta_0^{12/5})^{-5/6}}{1 + 0.90d_R^2 + 0.62d_R^2\beta_0^{12/5}}\right] - 1.$$

Incident spherical wave—if a spherical wave illuminates a diffuse (Lambertian) target of radius W_R, the **scintillation index** associated with the echo wave in a **monostatic channel** is

$$\sigma_I^2(0, 2L)_{\text{monostatic}} = \sigma_{\text{diff}}^2(L)\left[2 + \sigma_{\text{diff}}^2(L)\right] + \frac{2\sigma_{\text{diff}}^2(L)}{[1 + \sigma_{I,\text{sph}}^2(L)]^2}\left\{1 + \sigma_{\text{diff}}^2(L)\left[2 + \sigma_{\text{diff}}^2(L)\right]\right\},$$

where

$$\sigma_{I,\text{sph}}^2(L) = \exp\left[\frac{0.49\beta_0^2}{(1 + 0.56\beta_0^{12/5})^{7/6}} + \frac{0.51\beta_0^2}{(1 + 0.69\beta_0^{12/5})^{5/6}}\right] - 1.$$

Scintillation Index: Diffuse Target—II

Here we assume the characteristic correlation time τ_c associated with fluctuations in surface irregularities in the target is much longer than the time constant τ_d of the detector (i.e., $\tau_c \gg \tau_d$).

Incident spherical wave—if a spherical wave illuminates a diffuse (Lambertian) target of radius W_R, the **scintillation index** associated with the echo wave in a bistatic channel is

$$\sigma_I^2(r, 2L)_{\text{bistatic}} = 1 + 2\sigma_{\text{diff}}^2(L)[2 + \sigma_{\text{diff}}^2(L)], \quad r \gg \sqrt{L/k}.$$

Incident spherical wave—if a spherical wave illuminates a diffuse (Lambertian) target of radius W_R, the **scintillation index** associated with the echo wave in a monostatic channel is

$$\begin{aligned}\sigma_I^2(0, 2L)_{\text{monostatic}} &= 1 + 2\sigma_{\text{diff}}^2(L)[2 + \sigma_{\text{diff}}^2(L)] \\ &\quad + \frac{4\sigma_{\text{diff}}^2(L)}{[1 + \sigma_{I,\text{sph}}^2(L)]^2}\{1 + \sigma_{\text{diff}}^2(L)[2 + \sigma_{\text{diff}}^2(L)]\}.\end{aligned}$$

Strong irradiance fluctuations—in the saturation regime, the scintillation index approaches the asymptotic results

$$\sigma_I^2(r, 2L) \cong \begin{cases} 7 + \dfrac{15.12}{\beta_0^{4/5}}, \quad \beta_0^2 \gg 1 \\ \quad \text{bistatic channel: } r \gg \sqrt{L/k} \\ 11 + \dfrac{22.8}{\beta_0^{4/5}}, \quad \beta_0^2 \gg 1 \\ \quad \text{monostatic channel: } r = 0 \end{cases}$$

Equation Summary

Kolmogorov turbulence (structure function and power spectrum):

$$D_n(R) = C_n^2 R^{2/3}, \quad l_0 \ll R \ll L_0 \qquad \Phi_n(\kappa) = 0.033 C_n^2 \kappa^{-11/3}$$

Gaussian-beam wave in free space:

$$U_0(r,0) = A_0 \exp\left(-\frac{r^2}{W_0^2} - \frac{ikr^2}{2F_0}\right)$$

$$U_0(\mathbf{r},L) = A \exp\left(-\frac{r^2}{W^2} - i\frac{kr^2}{2F}\right) \times \exp\left(ikL - i\tan^{-1}\frac{\Lambda_0}{\Theta_0}\right)$$

$$A = A_0/\sqrt{\Theta_0^2 + \Lambda_0^2} \quad \Theta_0 = 1 - L/F_0 \quad \Lambda_0 = 2L/kW_0^2$$

$$W = W_0(\Theta_0^2 + \Lambda_0^2)^{1/2} \quad F = \frac{F_0(\Theta_0^2 + \Lambda_0^2)(\Theta_0 - 1)}{(\Theta_0^2 + \Lambda_0^2 - \Theta_0)}$$

Rytov approximation:

$$U(\mathbf{r},L) = U_0(\mathbf{r},L)\exp[\psi(\mathbf{r},L)] = U_0(\mathbf{r},L)\exp[\psi_1(\mathbf{r},L) + \psi_2(\mathbf{r},L) + \cdots]$$

Extended Huygens-Fresnel Principle:

$$U(\mathbf{r},L) = -\frac{ik}{2\pi L}\exp(ikL)\iint_{-\infty}^{\infty} d^2s\, U_0(\mathbf{s},0) \times \exp\left[\frac{ik|\mathbf{s}-\mathbf{r}|^2}{2L} + \psi(\mathbf{r},\mathbf{s})\right]$$

Mutual coherence function (beam spot size, beam wander, and spatial coherence):

$$W_e = W\sqrt{1 + 1.63\sigma_1^{12/5}\Lambda} \quad \sigma_1^2 = 1.23 C_n^2 k^{7/6} L^{11/6}$$

$$\langle r_c^2\rangle^{1/2} = \sqrt{W_e^2 - W_{ST}^2} = \sqrt{2.42 C_n^2 L^3 W_0^{-1/3}}$$

$$\rho_0 \equiv \rho_{\text{pl}} = (1.46 C_n^2 k^2 L)^{-3/5}, \quad l_0 \ll \rho_0 \ll L_0 \quad (r_0 = 2.1\rho_0)$$

Equation Summary

Scintillation index (plane wave, spherical wave, Gaussian-beam wave):

$$\sigma_I^2 = \exp\left[\frac{0.49\sigma_1^2}{(1+1.11\sigma_1^{12/5})^{7/6}} + \frac{0.51\sigma_1^2}{(1+0.69\sigma_1^{12/5})^{5/6}}\right] - 1,$$

$$0 \le \sigma_1^2 < \infty$$

$$\sigma_I^2 = \exp\left[\frac{0.49\beta_0^2}{(1+0.56\beta_0^{12/5})^{7/6}} + \frac{0.51\beta_0^2}{(1+0.69\beta_0^{12/5})^{5/6}}\right] - 1,$$

$$0 \le \beta_0^2 < \infty$$

$$\beta_0^2 = 0.4\sigma_1^2 = 0.5C_n^2 k^{7/6} L^{1/6}$$

$$\sigma_I^2(r,L) = 4.42\sigma_1^2\left(\frac{\Lambda}{1+1.63\sigma_1^{12/5}\Lambda}\right)\frac{r^2}{W(1+1.63\sigma_1^{12/5}\Lambda)}$$

$$+ \exp\left[\frac{0.49\sigma_B^2}{(1+0.56(1+\Theta)\sigma_B^{12/5})^{7/6}}\right.$$

$$\left. + \frac{0.51\sigma_B^2}{(1+0.69\sigma_B^{12/5})^{5/6}}\right] - 1,$$

$$0 \le \sigma_1^2 < \infty.$$

$$\sigma_B^2 = 3.86\sigma_1^2 \operatorname{Re}\left[i^{5/6}\,{}_2F_1\left(-\frac{5}{6}, \frac{11}{6}; \frac{17}{6}; \overline{\Theta} + i\Lambda\right) - \frac{11}{16}\Lambda^{5/6}\right]$$

Covariance function (plane wave):

$$B_I(\rho) = \exp\left[\frac{0.49\sigma_1^2}{(1+1.11\sigma_1^{12/5})^{7/6}}\,{}_1F_1\left(\frac{7}{6}; 1; -\frac{k\rho^2\eta_x}{4L}\right)\right.$$

$$\left. + \frac{0.50\sigma_1^2}{(1+0.69\sigma_1^{12/5})^{5/6}}\left(\frac{k\rho^2\eta_y}{L}\right)^{5/12} K_{5/6}\left(\sqrt{\frac{k\rho^2\eta_y}{L}}\right)\right] - 1$$

$$\rho_c = \begin{cases} \sqrt{L/k}, & \sigma_1^2 < 1 \\ \rho_0, & \sigma_1^2 \gg 1 \end{cases}$$

Equation Summary

Aperture averaging, flux variance (plane wave and spherical wave):

$$A = \frac{\sigma_I^2(D)}{\sigma_I^2(0)} = \left[1 + 1.06\left(\frac{kD^2}{4L}\right)\right]^{-7/6}, \quad \sigma_1^2 < 1$$

$$\sigma_I^2(D) \cong \exp\left[\frac{0.49\sigma_1^2}{(1 + 0.65d^2 + 1.11\sigma_1^{12/5})^{7/6}} + \frac{0.51\sigma_1^2(1 + 0.69\sigma_1^{12/5})^{-5/6}}{1 + 0.90d^2 + 0.62d^2\sigma_1^{12/5}}\right] - 1, \quad 0 \le \sigma_1^2 < \infty$$

$$d = \sqrt{kD^2/4L}$$

$$\sigma_I^2(D) \cong \exp\left[\frac{0.49\beta_0^2}{(1 + 0.18d^2 + 0.56\beta_0^{12/5})^{7/6}} + \frac{0.51\beta_0^2(1 + 0.69\beta_0^{12/5})^{-5/6}}{1 + 0.90d^2 + 0.62d^2\beta_0^{12/5}}\right] - 1, \quad 0 \le \beta_0^2 < \infty$$

Imaging quantities:

$$r_0 = \left[0.42\sec(\zeta)k^2\int_0^L C_n^2(z)dz\right]^{-3/5}$$

$$\theta_0 = \frac{\cos^{8/5}(\zeta)}{\left[2.91k^2\int_{h_0}^H C_n^2(h)(h - h_0)^{5/3}dh\right]^{3/5}}$$

$$\tau_0 = \frac{\cos^{3/5}(\zeta)}{\left[2.91k^2\int_{h_0}^H C_n^2(h)V^{5/3}(h)dh\right]^{3/5}},$$

$$\mathrm{PSF}_0(r) = \left[\frac{J_1(Dr/2\lambda f)}{Dr/2\lambda f}\right]^2$$

$$\mathrm{MTF}_{\mathrm{atm}}(\nu) = \exp\left[-3.44(\lambda f\nu/r_0)^{5/3}\right]$$

Equation Summary

Spatial resolution:

$$d_{\text{Airy}} = 2.44\frac{\lambda f}{D} \qquad r_{\text{Airy}} = 1.22\frac{\lambda f}{D}$$

$$\theta_{\text{Rayleigh}} = 1.22\frac{\lambda}{D} \qquad \theta_{\text{Sparrow}} = \frac{\lambda}{D}$$

Strehl ratio and **long-exposure resolution**:

$$\text{SR} = \frac{1}{[1 + (D/r_0)^{5/3}]^{6/5}} \qquad \frac{R}{R_{\max}} \cong \frac{(D/r_0)^2}{[1 + (D/r_0)^{5/3}]^{6/5}}$$

Direct detection:

$$\text{Pr}_{\text{fa}} = \frac{1}{2}\,\text{erfc}\left(\frac{i_T}{\sqrt{2}\sigma_N}\right) \qquad \text{Pr}_{\text{d}} = \frac{1}{2}\,\text{erfc}\left(\frac{i_T - i_S}{\sqrt{2}\sigma_N}\right)$$

$$\text{Pr}(E) = \frac{1}{2}\int_0^\infty p_I(x)\,\text{erfc}\left(\frac{\langle \text{SNR}\rangle x}{2\sqrt{2}\langle i_S\rangle}\right)dx$$

Coherent detection:

$$\text{CNR}_0 = \frac{\epsilon\eta P_{S0}}{h\nu B} \qquad \langle \text{CNR}\rangle \cong \frac{\text{CNR}_0}{[1 + (D/r_0)^{5/3}]^{6/5}}$$

$$\left(\frac{S}{N}\right)_{\text{out}} = \frac{\langle \text{CNR}\rangle^2}{1 + 2\langle \text{CNR}\rangle + \sigma_I^2(D)\langle \text{CNR}\rangle^2}$$

Equation Summary

Fade statistics (lognormal model):

$$\Pr(I \le I_T) = \frac{1}{2}\left\{1 + \operatorname{erf}\left[\frac{\frac{1}{2}\sigma_I^2(r,L) + \frac{2r^2}{W_e^2} - 0.23F_T}{\sqrt{2}\sigma_I(r,L)}\right]\right\}$$

$$\langle n(I_T)\rangle = \nu_0 \exp\left[-\frac{\left(\frac{1}{2}\sigma_I^2(r,L) + \frac{2r^2}{W_e^2} - 0.23F_T\right)^2}{2\sigma_I^2(r,L)}\right]$$

$$\langle t(I_T)\rangle = \frac{\Pr(I \le I_T)}{\langle n(I_T)\rangle}$$

Enhanced backscatter (spherical wave and finite smooth target):

$$W_e = W_R\sqrt{(4+\Omega_R^2)\left[1 + 2.65\sigma_1^2\left(\frac{\Omega_R}{4+\Omega_R^2}\right)^{5/6}\right]}$$

$$\frac{\langle I(0,2L)\rangle}{I(0,2L)_{\text{uncorr}}} = \exp\left[0.4\sigma_1^2 - 2.65\left(\frac{\Omega_R}{4+\Omega_R^2}\right)^{5/6}\sigma_1^2\right], \quad \sigma_1^2 < 1$$

$$\Omega_R = 2L/kW_R^2$$

Enhanced backscatter (spherical wave and unresolved target):

$$\frac{\langle I(0,2L)\rangle}{I(0,2L)_{\text{uncorr}}} = \exp\left[\frac{0.49\beta_0^2}{(1+0.56\beta_0^{12/5})^{7/6}} + \frac{0.51\beta_0^2}{(1+0.69\beta_0^{12/5})^{5/6}}\right]$$

$$= \begin{cases} 1+\beta_0^2, & \beta_0^2 \ll 1 \\ 2 + \dfrac{1.89}{\beta_0^{4/5}}, & \beta_0^2 \gg 1 \end{cases}$$

Equation Summary

Scintillation index (double-pass, spherical wave, and unresolved target):

$$\sigma_I^2(r, 2L) = \begin{cases} \sigma_{I,\mathrm{sph}}^2(L)[2 + \sigma_{I,\mathrm{sph}}^2(L)], \\ \quad \text{(bistatic channel: } r \gg \sqrt{L/k}) \\ \sigma_{I,\mathrm{sph}}^2(L)[4 + \sigma_{I,\mathrm{sph}}^2(L)], \\ \quad \text{(monostatic channel: } r = 0) \end{cases}$$

$$\sigma_{I,\mathrm{sph}}^2(L) = \exp\left[\frac{0.49\beta_0^2}{(1 + 0.56\beta_0^{12/5})^{7/6}} + \frac{0.51\beta_0^2}{(1 + 0.69\beta_0^{12/5})^{5/6}}\right] - 1,$$

$$0 \le \beta_0^2 < \infty.$$

Scintillation index (double-pass, spherical wave, weak scintillations, and smooth target):

$$\sigma_I^2(0, 2L) = 15.44\sigma_1^2 \,\mathrm{Re}\left[i^{5/6}\, {}_2F_1\left(-\frac{5}{6}, \frac{11}{6}; \frac{17}{6}; \overline{\Theta}_2 + i\Lambda_2\right) - \frac{11}{16}\Lambda_2\right]$$

$$\Theta_2 = \frac{2}{4 + \Omega_R^2}, \quad \Lambda_2 = \frac{\Omega_R}{4 + \Omega_R^2}.$$

Scintillation index (double-pass, spherical wave, and diffuse target):

$$\sigma_{\mathrm{diff}}^2(L) = \exp\left[\frac{0.49\beta_0^2}{(1 + 0.18d_R^2 + 0.56\beta_0^{12/5})^{7/6}} + \frac{0.51\beta_0^2(1 + 0.69\beta_0^{12/5})^{-5/6}}{1 + 0.90d_R^2 + 0.62d_R^2\beta_0^{12/5}}\right] - 1.$$

Bibliography

Andrews, L. C. and R. L. Phillips, *Laser Beam Propagation through Random Media*, 2nd ed. (SPIE Press, Bellingham, WA, 2005).

Andrews, L. C., R. L. Phillips, and C. Y. Hopen, *Laser Beam Scintillation with Applications* (SPIE Press, Bellingham, WA, 2001).

Chernov, L. A., *Wave Propagation in a Random Medium* (McGraw-Hill, New York, 1960), trans. by R. A. Silverman.

Fante, R. L., "Electromagnetic beam propagation in turbulent media," *Proc. IEEE* **63**, 1669–1692 (1975).

Fante, R. L., "Electromagnetic beam propagation in turbulent media: an update," *Proc. IEEE* **68**, 1424–1443 (1980).

Ishimaru, A., *Wave Propagation and Scattering in Random Media* (IEEE Press, Piscataway, NJ, 1997); [previously published as Vols I & II by Academic, New York (1978)].

Jelalian, A. V., *Laser Radar Systems* (Artech House, Boston, 1992).

Kopeika, N. S., *A System Engineering Approach to Imaging* (SPIE Optical Engineering Press, Bellingham, WA, 1998).

Lambert, S. G., and W. L. Casey, *Laser Communications in Space* (Artech House, Boston, 1995).

Lawrence, R. S., and J. W. Strohbehn, "A survey of clear-air propagation effects relevant to optical communications," *Proc. IEEE* **58**, 1523–1545 (1970).

Prokhorov, A. M., F. V. Bunkin, K. S. Gochelashvily, and V. I. Shishov, "Laser irradiance in turbulent media," *Proc. IEEE* **63**, 790–809 (1975).

Rytov, S. M., Yu. A. Kravtsov, and V. I. Tatarskii, "Principles of statistical radiophysics," in *Wave Propagation Through Random Media* (Springer, Berlin, 1989), Vol. 4.

Bibliography (cont'd)

Sasiela, R. J., *Electromagnetic Wave Propagation in Turbulence* (Springer, New York, 1994).

Tatarskii, V. I., *Wave Propagation in a Turbulent Medium* (McGraw-Hill, New York, 1961), trans. by R. A. Silverman.

Tatarskii, V. I., A. Ishimaru, and V. U. Zavorotny, eds., *Wave Propagation in Random Media (Scintillation)* (SPIE Optical Engineering Press, Bellingham, Wash.; Institute of Physics Pub., Techno House, Bristol, England, 1993).

Siegman, A. E., *Lasers* (University Science, Mill Valley, CA, 1986).

Strohbehn, J. W., ed., *Laser Beam Propagation in the Atmosphere* (Springer, New York, 1978).

Uscinski, B. J., *The Elements of Wave Propagation in Random Media* (McGraw-Hill, New York, 1977).

Weichel, H., *Laser Beam Propagation in the Atmosphere* (SPIE Optical Engineering Press, Bellingham, WA, 1990).

Wheelon, A. D., *Electromagnetic Scintillation II: Weak Scattering* (Cambridge University Press, Cambridge, UK, 2003).

Zuev, V. E., *Laser Beams in the Atmosphere* (Consultants Bureau, New York, 1982), trans. by S. Wood.

Index

Index

Index

Index

Index

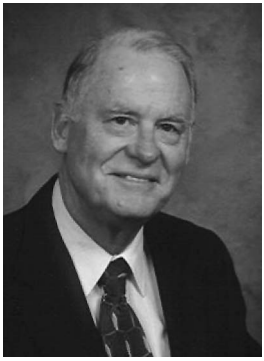

Larry C. Andrews is a Professor of mathematics at the University of Central Florida and an associate member of the College of Optics/CREOL. He is also an associate member of the Florida Space Institute (FSI). Previously, he held a faculty position at Tri-State University and was a staff mathematician with the Magnavox Company, antisubmarine warfare (ASW) operation. He received a doctoral degree in theoretical mechanics in 1970 from Michigan State University. Dr. Andrews has been an active researcher in optical wave propagation through random media for more than 20 years and is the author or co-author of 10 textbooks on differential equations, boundary value problems, special functions, integral transforms, and wave propagation through random media. Along with wave propagation through random media, his research interests include special functions, random variables, atmospheric turbulence, and signal processing.